MCB
Journals.ASM.org

Cdyl, a New Partner of the Inactive X Chromosome and Potential Reader of H3K27me3 and H3K9me2

M. Escamilla-Del-Arenal,[a] S. T. da Rocha,[a] C. G. Spruijt,[b] O. Masui,[a]* O. Renaud,[a,c] Arne H. Smits,[b] R. Margueron,[d] M. Vermeulen,[b] E. Heard[a]

Mammalian Developmental Epigenetics Group, Institut Curie, CNRS UMR 3215, INSERM U934, Paris, France[a]; Department of Molecular Cancer Research, University Medical Center Utrecht, Utrecht, The Netherlands[b]; PICT-IBiSA, Institut Curie, Centre de Recherche, Paris, France[c]; Mechanisms of Repression by Polycomb Proteins Group, Institut Curie, CNRS UMR 3215, INSERM U934, Paris, France[d]

X chromosome inactivation is a remarkable example of chromosome-wide gene silencing and facultative heterochromatin formation. Numerous histone posttranslational modifications, including H3K9me2 and H3K27me3, accompany this process, although our understanding of the enzymes that lay down these marks and the factors that bind to them is still incomplete. Here we identify Cdyl, a chromodomain-containing transcriptional corepressor, as a new chromatin-associated protein partner of the inactive X chromosome (Xi). Using mouse embryonic stem cell lines with mutated histone methyltransferase activities, we show that Cdyl relies on H3K9me2 for its general association with chromatin *in vivo*. For its association with Xi, Cdyl requires the process of differentiation and the presence of H3K9me2 and H3K27me3, which both become chromosomally enriched following Xist RNA coating. We further show that the removal of the PRC2 component Eed and subsequent loss of H3K27me3 lead to a reduction of both Cdyl and H3K9me2 enrichment on inactive Xi. Finally, we show that Cdyl associates with the H3K9 histone methyltransferase G9a and the MGA protein, both of which are also found on Xi. We propose that the combination of H3K9me2 and H3K27me3 recruits Cdyl to Xi, and this, in turn, may facilitate propagation of the H3K9me2 mark by anchoring G9a.

In mammals, dosage compensation for X-linked gene products between XX females and XY males is achieved by the inactivation of one of the two X chromosomes in females, a phenomenon known as X chromosome inactivation (XCI) (1). XCI is triggered by the noncoding Xist transcript, which is expressed from one of the two X chromosomes during early development, coats the chromosome from which it is produced in *cis*, and initiates gene silencing, as well as a number of chromatin changes (see reference 2 for a review). Once established, the inactive X chromosome (Xi) remains silent through subsequent cell divisions and represents a dramatic example of epigenetic silencing in eukaryotes. Although the initiation of XCI has been studied extensively, the protein factors that participate in silencing and its maintenance are unknown.

Mouse embryonic stem cells (mESCs), derived from female blastocysts, are a useful model system for investigating XCI, as they recapitulate this process when differentiation is induced *in vitro*. During female ESC differentiation, *Xist* becomes monoallelically upregulated on one X chromosome and triggers gene silencing of that chromosome. Chromatin marks associated with active transcription, such as H3K4 methylation, rapidly become globally depleted on the Xist RNA-coated X chromosome (3–6). Following this, several proteins and histone marks correlated with gene silencing become enriched on Xi. Facultative heterochromatin of Xi is progressively formed during differentiation, with transcriptional repression being gradually locked in, presumably because of synergy between the different chromatin changes (7). However, the exact mechanisms by which this chromosome-wide gene silencing process is initiated and then stably maintained remain poorly understood.

The Polycomb group (PcG) complexes are probably the best-characterized protein complexes associated with Xi. PRC2 recruitment to Xi results in trimethylation of histone H3 lysine 27 (H3K27me3) (8–10), while PRC1 recruitment catalyzes the monoubiquitination of histone H2A lysine 119 (H2AK119ub1) of Xi (11, 12). PRC2 is thought to be recruited to Xi via Xist RNA, either directly or indirectly (10, 13). Different PRC1 complexes are recruited to Xi in at least two ways: via CBX7 binding to the H3K27me3 mark (14, 15) and via RYBP, independently of H3K27me3 and CBX7 (16, 17). The complexes that lay down or associate with the other histone modifications on Xi are less well characterized. The H3K9me2 (3) and H4K20me1 (18) marks become enriched on the Xist RNA-coated chromosome within the same time window as PRC2 and PRC1, although it is not clear whether these changes are linked to or downstream of the PcG complexes on Xi or whether they occur independently of PcG (16). The H4K20me1 mark is dependent on the histone methyltransferase (HMT) PRSet7. The absence of this protein rapidly leads to cell death and embryonic lethality (19). The HMT responsible for H3K9me2 enrichment on Xi is unclear. Several H3K9 HMTs, including G9a and ESET, may be involved, with a certain degree of redundancy, but this has so far not been established.

An important question is whether the histone modifications that become enriched on Xi have a role, either alone or in combination, in recruiting factors that participate in the process of XCI.

Received 9 July 2013 Returned for modification 18 August 2013
Accepted 11 October 2013
Published ahead of print 21 October 2013
Address correspondence to E. Heard, Edith.Heard@curie.fr, or M. Vermeulen, M.Vermeulen-3@umcutrecht.nl.
* Present address: O. Masui, Laboratory for Developmental Genetics, Research Centre for Allergy and Immunology, RIKEN Yokohama Institute, Tsurumi, Yokohama, Kanagawa, Japan.
Copyright © 2013, American Society for Microbiology. All Rights Reserved.
doi:10.1128/MCB.00866-13

Recently, the chromodomain-containing transcriptional corepressor protein Cdyl was reported to bind H3K9me3- and H3K27me3-containing histone peptides (20) and to have a high affinity for the H3K9me2 modification (21). Furthermore, CDYL is able to bind to reconstituted nucleosomes carrying the H3K9me3 mark (22). Cdyl could therefore be a candidate effector ("reader") protein of the histone H3K9 and K27 methylation marks associated with Xi. Cdyl belongs to the Cdy (chromodomain Y) family (23), which represents a set of related genes in higher eukaryotes (24). In humans, the CDY family comprises two autosomal genes, *CDYL1* and *CDYL2*, as well as multiple copies of the *CDY* gene, on the Y chromosome (24). Three splicing variants of CDYL1 (CDYL1a, -b, and -c) have been described that differ in the N-terminal domain (21). The CDYL1b variant has been shown to depend on protein multimerization in order to interact with the H3K9me3 mark *in vitro* (21). In the mouse, two related genes, *Cdyl* and *Cdyl2*, have been identified (23). In addition to its chromodomain, which may mediate H3K9me3 and/or H3K27me3 binding, Cdyl harbors an enoyl coenzyme A (CoA) hydratase (ECH) homology domain of unknown function that has been shown to bind CoA and the histone deacetylases Hdac1 and Hdac2, suggesting that Cdyl is primarily a transcriptional corepressor (25). Biochemical studies have suggested that Cdyl recruits G9a to REST targets (26) and that it has a possible role in PRC2 recruitment via the H3K27me3 mark (27). Altogether, these studies point to the participation of Cdyl in several chromatin-modifying and gene regulatory processes.

Here, we show that Cdyl is a developmentally and cell cycle regulated protein that becomes associated with Xi early on in XCI. This association appears to be dependent on the onset of cellular differentiation and the combined presence of the H3K9me2 and H3K27me3 histone marks. We also demonstrate that Cdyl-deficient mESCs are viable but have a compromised ability to differentiate and die rapidly upon differentiation. Finally, we identify several Cdyl interacting partners and provide evidence that some of these can associate with Xi, including H3K9me2 HMT G9a. Our study provides one of the first examples of how combinatorial histone modifications on Xi may serve as a specific binding platform for chromatin state "readers" that can, in turn, recruit additional effector proteins, some of which may participate in the propagation of the chromatin state itself.

MATERIALS AND METHODS

Cell culture. Female LF2 and PGK12.1 ESCs were grown under feeder-free conditions in gelatin-coated flasks in classical ES medium as previously described (6). Male ESC lines 36:11 (28), ΔSX (29), and 36:11 *Eed*$^{-/-}$ (16) were grown on a feeder layer in gelatin-coated flasks as previously described (28). Male TT2, *G9a*$^{-/-}$ (30), and *Eed*$^{-/-}$ (31) ESCs were grown on a feeder layer in gelatin-coated flasks under the same conditions as feeder-free ESCs. Differentiation was induced by preadsorbing feeders in the case of feeder-dependent ESCs, removing leukemia inhibitory factor (LIF), and applying 100 nM all-*trans*-retinoic acid (Sigma) in Dulbecco's modified Eagle's medium containing 10% fetal bovine serum and 10^{-4} mM 2-mercaptoethanol. Embryoid body differentiation was performed by standard procedures.

Cdyl expression constructs. The Cdyl-green fluorescent protein (GFP) fusions that were used in transient transfections were generated by PCR from the *Cdyl* cDNA (25) and inserted into vectors pEGFP-N2 and pEGFP-C2 (BD Biosciences Clontech). For the Cdylb and Cdylc variants or specific Cdyl domains, PCR amplification was used to add or eliminate specific domains and PCR products were inserted into vectors pEGFP-N2 and pEGFP-C2 (the primers used are described below). For Cdyl-GFP stable cell lines, GFP-Cdyl constructs were introduced into the pBROAD3-mcs (InvivoGene) plasmid and stably transfected into ESCs. A hygromycin cassette was integrated into plasmid pBROAD3 as a selectable marker for ESC clone selection. The hygromycin cassette was generated by PCR amplification adding NdeI restriction sites and integrated into the VspI site from pBROAD3. Clone selection was carried out with a hygromycin concentration of 250 μg/ml. For Cdyl knockdowns, the 5′-GAGA TATTGTCGTCAGGAA-3′ and 5′-CAGTTCTGATCAAACTTAA-3′ sequences were introduced into pSuper.puro (Oligoengine) and stably transfected in accordance with the manufacturer's specifications. Clone selection was performed with 1 μg/ml puromycin.

RNA FISH and IF assays. Xist RNA fluorescence *in situ* hybridization (FISH) was performed with a 19-kb genomic lambda clone (510) probe labeled by nick translation (Vysis) with Spectrum Red-dUTP, Spectrum Cy5-dUTP, or Spectrum Green-dUTP in accordance with the manufacturer's instructions. Immunofluorescence (IF) assays and RNA FISH were performed as described previously (32). For precleared IF assay-FISH experiments, a permeabilization step with 0.1 g/ml digitonin (Sigma) was add before the standard IF assay-FISH fixation. In brief, cells were washed with phosphate-buffered saline and permeabilized with CSK buffer containing 0.1 g/ml digitonin (Sigma) for 5 min at 4°C, digitonin was washed out with CSK buffer, and cells were fixed in 3% paraformaldehyde. From this step, the protocols are the same as for a standard IF assay. The antibodies used were as follows: Cdyl, IF-1/100 and WB-1/1000 (Abcam; lot 419777; rabbit); H3K9me2, IF-1/100 and WB-1/2000 (Cosmo Bio; mouse); H3K27me3, IF-1/300 and WB-1/2000 (gift from D. Reinberg [33]; mouse); H3S10p, IF-1/250 (Upstate; mouse); G9a, IF-1/100 and WB-1/2000 (Cell Signaling; rabbit); Mier1, IF-1/100 and WB-1/500 (Santa Cruz; goat); HMGA1a/HMGA1b, IF-1/100 and WB-1/1000 (Abcam; rabbit); GFP, IF-1/100 and WB-1/3000 (Abcam; rabbit); REST/NRSF, IF-1/100 and WB-1/2000 (Abcam; rabbit); Eed, IF-1/5 (gift from A. P. Otte [34]; mouse); Ring1b, IF-1/100 (MBL; mouse); HDAC1, WB-1/2000 (Active Motif; mouse); HDAC2, WB-1/2000 (Abcam; mouse); polII, WB-1/3000 (Abcam; rabbit); Ezh2, WB-1/3000 (gift from D. Reinberg [35]; mouse).

Imaging. Fluorescence imaging was undertaken with either a DeltaVision microscope (Applied Precision) or an Apotome microscope (Zeiss).

Transient and stable transfections. Stable ESC lines were generated by using Lipofectamine 2000 (Invitrogen) under the conditions recommended by the manufacturer and then grown under selection under standard conditions. Transient transfections were performed with *Trans*IT-LT1 (Euromedex) in accordance with the manufacturer's recommendations.

Tet-inducible Cbx7-EGFP cell line. The female mESC line LF2 was electroporated with a linearized pROSA26/P-nlsrtTA plasmid to generate the cell line LF2/P-ROSA26-rtTA, which stably expresses rtTA at the ROSA26 locus. LF2 and pROSA26/P-nlsrtTA were gifts from Austin Smith and Philippe Soriano, respectively. To make a Tet-inducible Cbx7–enhanced-GFP (EGFP)-expressing plasmid, Cbx7 cDNA was fused with the EGFP open reading frame in frame and inserted into the BamHI/NotI site of pTRE-Tight (Clontech) to produce pTRE-Tight/Cbx7-EGFP. Cbx7 cDNA was a gift from Jesus Gil. pTRE-Tight/Cbx7-EGFP was cotransfected with plasmid pL2-neo into LF2/P-ROSA26-rtTA cells, which were selected with 350 μg/ml G418 to generate the Tet-inducible Cbx7-EGFP-expressing ESC line. Clones with efficient Cbx7-EGFP induction upon 1 μg/ml doxycycline treatment were used for experiments.

RT-PCR. Total RNA was isolated from ESCs with TRIzol reagent (Invitrogen) and then DNase treated (Promega) to remove contaminating DNA. First-strand cDNA was prepared from 5 mg of RNA and random hexamers with Superscript III (Invitrogen) at 42°C for 1 h. Primer pairs (0.5 mM final concentration) were then used to amplify the sequence of interest with *Taq* DNA polymerase (Roche). For strand-specific reverse transcription (RT)-PCR, first-strand cDNA was prepared from 2.5 mg of RNA and 2 mM gene-specific primer in either the sense or the antisense orientation with Thermoscript enzyme (Invitrogen) at 62°C for 1 h. The primers used for the

transcriptional variants were Cdyl-C_up (GGTGGAATTCATGGGCATAG GCAATAGCCAGCCTAATTCA), mCdylTV2EcoRI_fwr (GGTGGAATTC ACCATGGCCTCCGAGGAGCTGTACGAGGTGGAAAGTATCGTTGAC AAAAG), mCdylTV3EcoRI_fwr (GGTGGAATTCACCATGGACCTCGCC AAGTCAGG), Cdyl-C_lo (GCCCTCTAGAAGAACTCATCGATTTTCCT CTGTAAGT), CdylENO-C_up (GGTGGAATTCATGGCCACAGGCTTA GCTGTTAATGGA), Cdylchrom-C_lo (GCCCTCTAGACTTTTCCATTA ACAGCTAAGCCTGTGG), and Cdyl-C_lo (GCCCTCTAGAAGAACTCA TCGATTTTCC TCTGTAAGT). The RT primers used for transcriptional-variant analysis were mCdylTV1_fwr (CAAGACGCGGAGACTCAG), mCdylTV1/2_rev (GATGTATTCCTCACAGTTCAC), mCdylexon3/4_fwr (CCAGCTCTGCACACTTCC), mCdylexon3/4_rev (CTGAGTCTCCGCG TCTTG), mCdylexon5/6_fwr (GCTTTGCTGGGCCCTGG), mCdylexon5/ 6_rev (CTAGCGCATCCATGAATGG), mCdylexon6/7_fwr (CACCCACA TCTTGTTATCCAC), mCdylexon6/7_rev (GTCCAGACCACAGCAGA AG), mCdylexon7/8_fwr (GACCGAAAGAGAGAAAGCAC), mCdylexon7/ 8_rev (ACAAAGAGGCAATATGGATGC), mCdylTV3ex1_1_fwr (GTAGA TGGCATGCAGATTATTG), mCdylTV3ex1_2_fwr (GAGAGAGAAAGAAG GGAGGG), mCdylTV3ex1_ 3_fwr (CTGTTTGAATCTCCTCCACTG), mCdylTV3ex2_1_fwr (TGATGTTGGTGGAGGTGG), mCdylTV3ex1_1_rev (CAGTGGAGGAGATTCAAACAG), mCdylTV3ex1_2 _rev (GGTATGGAAG TGGTCAACATG), mCdylTV3ex2_1_rev (CAGGCTTTGAGGACCCTTC), and mCdylTV3ex2_2_rev (CCTGACTTGGCGAGGTC).

WB analysis. Whole-cell extracts were prepared with conventional radioimmunoprecipitation assay buffer, and high-salt (HS) nuclear extracts and chromatin fractions were generating by using a cell fractionation protocol. Briefly, fractions were separated by cell centrifugation and the use of hypertonic buffer (10 mM Tris-HCl [pH 7.9], 10 mM KCl, 0.1 mM EDTA, 0.1 mM EGTA) and HS buffer (50 mM Tris-HCl [pH 7.5], 10% sucrose, 420 mM KCl, 0.1 mM EDTA, 5 mM $MgCl_2$, 20% glycerol). Protease inhibitors were added. For Western blotting (WB), extracts were loaded and electrophoresed by SDS-PAGE with 8 to 12% gradient gels. WB analyses were performed by following the protocols provided by each antibody supplier and detected with the Amersham ECL+ detection kit by using horseradish peroxidase-conjugated secondary antibodies according to the manufacturer's recommendations.

Nuclear extracts. Cells were cultured as described above. Nuclear extracts were prepared essentially as described in reference 36. Cells were harvested and swollen in a hypotonic buffer, after which they were lysed by Dounce homogenization. Nuclei were lysed by resuspending the pellet in 2 volumes of 420 mM NaCl–20 mM HEPES (pH 7.9)–20% (vol/vol) glycerol–2 mM $MgCl_2$–0.2 mM EDTA–0.1% NP-40–complete protease inhibitor without EDTA (Roche)–0.5 mM dithiothreitol (DTT) and then incubating it in a rotation wheel for 1 h at 4°C. After centrifugation, the supernatant contained the soluble nuclear proteins. Protein concentrations were determined by Bio-Rad protein assay.

Label-free GFP affinity purifications. GFP affinity purifications were performed essentially as described in reference 53. Pulldowns were performed in triplicate with 7.5 μl of GFP binder beads (Chromotek GFP_Trap_A) (both CDYL-specific purification and wild-type [WT] control) or blocked agarose beads (Chromotek, bab-20) (NON-GFP bead control). One milligram of nuclear extract was diluted with incubation buffer (300 mM NaCl, 20 mM HEPES KOH [pH 7.9], 20% [vol/vol] glycerol, 2 mM $MgCl_2$, 0.2 mM EDTA, 0.1% NP-40, 0.5 mM DTT, complete protease inhibitors) to a final volume of 400 μl. Ethidium bromide at a final concentration of 50 μg/ml was added to prevent indirect, DNA-mediated interactions. After a 90-min incubation in a rotation wheel at 4°C, beads were washed extensively and bound proteins were finally subjected to on-bead trypsin digestion (38). Peptides were desalted and concentrated with Stagetips (39).

Mass spectrometry. Peptides were separated by high-performance liquid chromatography with an EASY-nLC system (Proxeon) connected online to an LTQ-Orbitrap-Velos (Thermo) mass spectrometer. Spectra were recorded in collision-induced dissociation mode, during a 120-min gradient of organic solvent (5 to 30% acetonitrile), and the 15 most abundant peptides were fragmented for tandem mass spectrometry. Raw data were analyzed with the free MaxQuant package, version 1.2.2.5, and the ipi.MOUSE.v3.68.fasta protein database. With Perseus, data were filtered for contaminants, reverse hits, the number of peptides (>1), and unique peptides (>0). Label-free quantification (LFQ) intensities were converted to logarithmic values (log_2). After "groups" were defined, filtering was performed on the basis of valid values, with at least three values in a single group, assuming that CDYL-specific interactors may not be identified in the control pulldowns. The missing values were computed by using a normal distribution (width = 0.3, shift = 1.8). The significant outliers were calculated by using *t* tests for CDYL versus control groups (tv = 0.0001, S0 = 4), in which multiple-testing correction was applied by using a permutation-based false-discovery rate (FDR) method. Volcano plots were made by using R with the curve resulting from the *t* test, in which the LFQ ratio of the Cdyl to the control purification is plotted on the *x* axis and the *P* value of the *t* test is plotted on the *y* axis.

Photobleaching experiments. A Zeiss LSM780 confocal microscope was used for all photobleaching experiments. Fluorescence recovery after photobleaching (FRAP) was performed with GaAsP detectors and the 488-nm line of a 25-mW argon laser. The bleaching time was 600 ms with 1.9 mW of power at the back focal plane of the objective. The bleach region was a circle with a diameter of 10 pixels, and a pixel dwell of 2 μs and 100 iterations were used. All experiments were done at 37°C, and imaging was done with an alpha-plan Apochromat 1.46 numerical aperture 63× objective. Scanning was monodirectional with a zoom of 5 and a 488-nm laser line at 1.1% (7.3 μW at the back focal plane of the objective). During the recovery period, 190 images (128 by 128 pixels) were collected every 500 ms until the recovery signal reached a plateau. Identical imaging settings were used for all prebleach (10 images) and postbleach experiments. Photobleaching was measured for each cell and was low. Image analysis was performed with Zen 2011 (Zeiss software) for intensity measurement, FRAPcalc software (Kota Miura, Center for Molecular and Cellular Imaging, EMBL Heidelberg) in IgorPro (WaveMetrics) for curve fitting (double-exponential model with double normalization) and mobile fraction and half-maximal value estimation, and Excel (Microsoft) for graphs.

RESULTS

Identification of Cdyl as a new protein partner of Xi in early embryonic lineages. In a previous study, Cdyl was identified as a binding protein for both H3K9me3 and H3K27me3 (20). Using quantitative mass spectrometry based on stable isotope labeling with amino acids in cell culture (SILAC) and WB analysis, we found that Cdyl also binds to H3K9me2 (Fig. 1A and B). These findings prompted us to consider Cdyl as a candidate binding protein or "reader" that might be recruited to H3K9me2/H3K27me3-enriched Xi. Using IF assays with an anti-Cdyl antibody combined with Xist RNA FISH, we examined whether Cdyl is associated with Xi in different mouse cell types representing different lineages, including female mESCs before and after differentiation, primitive endoderm (XEN) cells (which contain an inactive paternal X chromosome, Xp), trophoblast stem cells (also contain inactive Xp), as well as primary mouse embryonic fibroblasts (MEFs), which contain an inactive paternal or maternal X chromosome and are thought to represent a later stage of differentiation. In all of the cell lines examined, Cdyl was found to colocalize with Xi in a proportion of the cells (Fig. 1C). This colocalization was seen with two different antibodies raised against Cdyl and tested in both mouse and human (HEK293) cells (data not shown). Taken together, these results identify Cdyl as a new partner of Xi.

Cdyl enrichment (defined as a greater intensity of staining than the rest of the nucleus) on the Xist RNA-coated chromosome was

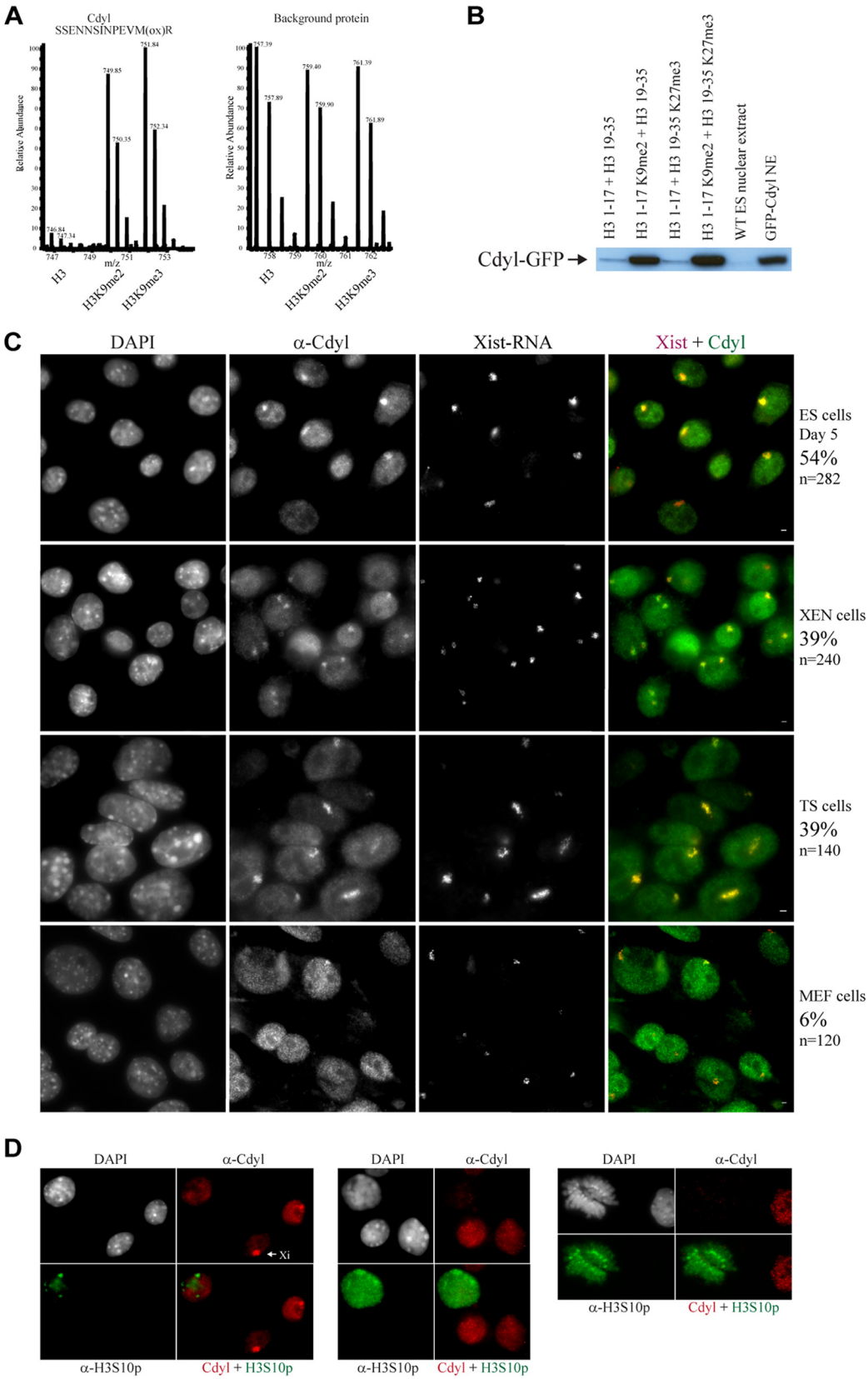

FIG 1 Recruitment of the Cdyl protein to Xi. (A) SILAC-based histone peptide pulldown approach (59). Representative spectra of a Cdyl peptide showing higher intensity in the heavy form, demonstrating specific H3K9me2/3 binding. (B) The preferential interaction was confirmed by pulldowns of nuclear extracts with unmodified H3, H3K9me2, H3K27me3, or a mixture of the peptides. Bound proteins were analyzed by immunoblotting with anti-GFP antibodies. (C) Cdyl enrichment on Xi was determined by IF assay with an anti-Cdyl antibody (green in merged image) combined with Xist RNA FISH (red in merged image). DNA was stained with 4,6-diamidino-2-phenylindole (DAPI). An analysis of different mouse cell lines representative of the first three embryonic lineages was performed. The percentage of enrichment is shown in relation to the total number of cells. TS cells, trophoblast stem cells. (D) Cell cycle analysis of Cdyl by double IF assay of mESCs differentiated to day 5, with anti-Cdyl antibody staining (red) and anti-H3S10ph antibody staining (green). Cdyl is not present in the G_2/S phase of the cell cycle.

not detected in all cells, and in particular, it was absent from cells undergoing mitosis. This prompted us to consider cell cycle regulation of the Cdyl protein. We performed IF assay-FISH with an anti-histone H3 phosphoserine 10 (H3S10p) antibody (a characteristic mark at the onset of mitosis [40, 41]) and found that Cdyl staining was dramatically reduced in or absent from H3S10p-positive cells (Fig. 1D). Thus, nuclear Cdyl protein is present only in the G_1/S and not in the G_2/M phase of the cell cycle. This is consistent with biochemical data showing that binding of Cdyl to H3K9me3 is negatively affected by H3S10p (20, 21) and expression data showing that CDYL is downregulated about 3-fold in mitosis (42). In summary, our data reveal that Cdyl is a novel protein partner of Xi that is recruited during the onset of XCI. Cdyl is present in the three earliest embryonic mouse lineages, as well as in transformed cells, and is less abundant in fully differentiated cells.

The Cdylb splice variant is recruited to the Xist RNA-coated X chromosome during early ESC differentiation. We next evaluated the timing of Cdyl recruitment to the X chromosome during ESC differentiation and XCI. By performing anti-Cdyl IF assays combined with Xist RNA FISH (Fig. 2A), Cdyl was first found to be enriched on the Xist RNA-coated chromosome at day 2 of differentiation, which corresponds to the time when gene silencing begins and chromatin changes such as H3K9me2 and H3K27me3 enrichment appear on Xi (3, 10, 33, 43). Interestingly, the highest proportion of cells with Xi enriched for Cdyl was found at around day 5 of differentiation. The proportion decreased at later stages, suggesting that enrichment of this protein on Xi is transient during development. Indeed, in more differentiated cell types, such as MEFs, only a very low percentage (~6%) of the cells displayed Cdyl enrichment on Xi (Fig. 1C). We also examined Cdyl protein and RNA levels during differentiation by WB analysis (Fig. 2B) and RT-PCR (Fig. 2C), respectively. Cdyl RNA and protein were observed to be present throughout ESC differentiation, with only a slight increase at later stages. We therefore conclude that the recruitment of Cdyl to Xi between days 2 and 5 of differentiation is associated primarily with the changing chromatin status (enrichment for H3K9 and H3K27 methylation) of the Xist RNA-coated chromosome. The decrease in Cdyl association with Xi at later stages of differentiation correlates with the decrease in Xi enrichment of H3K9 and H3K27 methylation (33).

Given that three alternatively spliced variants of CDYL1 (CDYL1a, -b, and -c) have been described in human cells (21), we wished to determine whether these also exist in mouse cells and if so, which of the variants associates with Xi. All three variants share the C-terminal enoyl-CoA hydratase-like domain, but only CDYL1a and -b contain the chromodomain and only CDYL1b can bind to H3K9me3 (21). The respective roles of these variants are still unclear. Using RT-PCR, we detected transcripts for all three putative Cdyl isoforms in mESCs (Fig. 2C). Transient transfections of the corresponding cDNAs fused to GFP into differentiating female mESCs revealed that Cdylb is the main isoform enriched on Xi (Fig. 2D). This was confirmed after stable transfection and analysis of transgenic ESC lines upon differentiation (Fig. 2E). The Xi association of Cdylb but not of Cdyla was consistent with studies of the human CDYLa and -b proteins and suggests that the 57-amino-acid Cdyla N-terminal extension inactivates the adjacent chromodomain and perturbs its interaction with H3K9 methylation. Further support for an inhibitory effect of the Cdyl N terminus on its binding to Xi came from our finding that an N-terminal GFP fusion of murine Cdylb severely affected its capacity to associate with Xi, unlike a C-terminal fusion (Fig. 2E).

To further investigate which domain(s) of the Cdylb protein is responsible for its recruitment to Xi, we stably transfected either full-length or truncated Cdylb (C-terminal GFP fusion) expression constructs into mESCs and induced differentiation. Only full-length Cdylb was able to associate with Xi during differentiation (Fig. 2F and G), suggesting that multiple portions of the Cdyl protein are required for its correct folding and/or recruitment to Xi. Finally, we noted that transfection of the Cdylc isoform had no impact on endogenous Cdyl recruitment to Xi (Fig. 2G). In conclusion, Cdylb appears to be the main isoform of Cdyl recruited to Xi. The amino- and carboxyl-terminal domains both appear to be required for this association, and expression of the other isoforms does not compete with Cdylb's Xi association.

Cdyl is enriched on Xi marked with H3K9me2 and H3K27me3. Given that Cdyl accumulation on Xi was found to occur within the same time window as the enrichment of H3K9me2 and H3K27me3 methylation (3, 10, 44) and that these marks are strong candidates for the recruitment of Cdyl to chromatin (Fig. 1 and reference 20), we explored whether they might be implicated in Cdyl's recruitment to Xi. We first analyzed the relative kinetics of enrichment of H3K9me2, H3K27me3, and Cdyl to the Xist RNA-coated X chromosome (Fig. 3). Using double IF assay-Xist RNA FISH with anti-Cdyl/anti-H3K27me3 or anti-Cdyl/anti-H3K9me2 antibodies, we found that H3K27me3 slightly precedes Cdyl enrichment (Fig. 3B), while Cdyl and H3K9me2 both start to be enriched on Xi in a proportion of the cells starting from day 2 (Fig. 3C). The proportion of H3K9me2/Cdyl-positive Xi cells peaks at day 5. Subsequently, both H3K9me2 and Cdyl decrease on Xi from day 5 to day 10 (Fig. 3D). In summary, Cdyl associates with Xi when both H3K27me3 and H3K9me2 are enriched on this chromosome, and Cdyl binding is lost when H3K9me2 enrichment diminishes on Xi. This suggests that a combination of H3K9me2 and H3K27me3 may be necessary for the recruitment of Cdyl to Xi and that the loss of Cdyl from Xi at later differentiation time points may be connected to the reduction of H3K9me2 levels on Xi. Finally, we noted that not all cells that were H3K9me2 or H3K27me3 positive during days 2 to 5 of differentiation were Cdyl positive. Presumably, this is due to cells that were in the G_2/M phase, where Cdyl is absent (Fig. 1D) although the chromatin marks on Xi persist.

Interaction of Cdyl with chromatin depends on the histone H3K9me2 mark. Given the correlation we found, we investigated whether the H3K9me2 and H3K27me3 marks might indeed be necessary for the recruitment of Cdyl to chromatin. For this, we used mESCs that lack either of these two marks because of disruption of the HMT responsible for them. Male mESCs were examined, as no female mutant mESCs were available. We first examined *Eed*$^{-/-}$ mESCs, which lack H3K27me3 (45) (Fig. 4A and D). Cdyl recruitment to chromatin was not obviously affected in IF analyses and only mildly affected in WB analysis (Fig. 4A to D), suggesting that H3K27me3 is not essential for Cdyl recruitment to chromatin.

Next, we examined mESCs lacking the H3K9me2 HMT, G9a, that were previously shown to lack global H3K9me2, at least in the undifferentiated state (30, 33). We studied the association of Cdyl with chromatin by IF assays and WB (Fig. 4B to D). The control parental cell line TT2 showed clear nuclear staining for both H3K9me2 and Cdyl (Fig. 4B, top). However, H3K9me2 staining

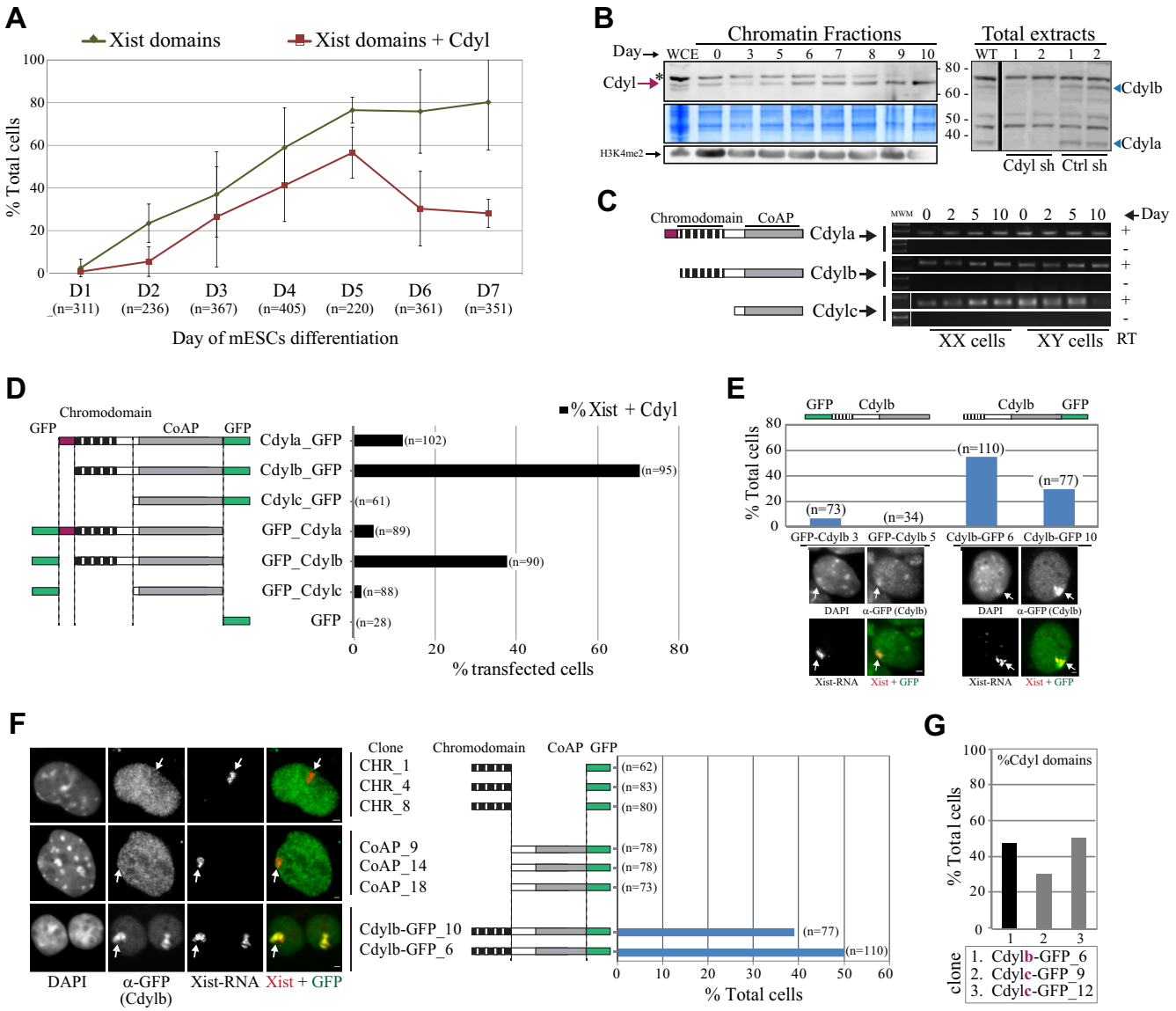

FIG 2 Cdylb is the major splice variant recruited to Xi. (A) Cdyl kinetics of enrichment on Xi in mESCs differentiated in the presence of RA as determined by anti-Cdyl IF assay-Xist RNA FISH experiments. Error bars correspond to standard deviations of four independent experiments. (B) Left, WB analysis of chromatin fractions from differentiated mESCs with anti-Cdyl antibody. Detection of anti-H3K4me2 antibody and Coomassie blue staining were used to control for loading. The red arrow shows the band corresponding to Cdyl, determined by WB in the Cdyl knockdown (right panel). WT, wild type; WCE, whole-cell extracts. The asterisk represents a nonspecific band. Right, WB analysis of nuclear extracts from Cdyl knockdown ESC lines with anti-Cdyl antibody. The arrowheads show the bands determined as corresponding to the Cdyl isoforms. Cdyl sh, shRNA against Cdyl; Ctrl sh, shRNA, control. The values in the center are molecular sizes in kilodaltons. (C) Schematic representation of the gene structure for the predicted splice variants of *Cdyl* in the mouse. CoA pocket (CoAP) domain illustrations and RT-PCR analysis show the presence of Cdyl splice variants Cdyla, -b, and -c in female (XX) and male (XY) cells across differentiation. MWM, molecular weight marker. (D) GFP was fused to the Cdyl splice variants and transiently transfected into PGK12.1 ESCs at day 3 of RA differentiation. The transfection efficiency averaged around 20%. Analysis was performed at day 5 of RA differentiation by IF assay with anti-GFP antibody combined with Xist RNA FISH. The percentage of Xi enrichment in transfected cells is shown. (E) Stable ESC lines were generated with constructs containing Cdylb fused to GFP at the N- and C-terminal domains. IF assay-FISH at day 5 with an anti-GFP antibody and Xist RNA shows that Cdyl-GFP is better recruited than GFP-Cdyl to Xi. Thee arrows indicate Xist domains. (F) Stable clonal cell lines were generated with constructs containing different domains of the Cdylb protein fused to GFP. IF assay-FISH at day 5 of RA differentiation shows that only the Cdylb-GFP full form is recruited to Xi. (G) Stable clonal cell lines were generated with constructs containing either Cdylb or Cdylc fused to GFP. In this cell line, the recruitment of the endogenous form of Cdyl to Xi was determined with anti-Cdyl antibody. The presence of Cdylc does not titrate endogenous Cdyl from Xi.

was totally absent from *G9a*$^{-/-}$ ESCs and Cdyl was no longer enriched in the nucleus, showing a diminished, dispersed signal (in contrast to WT feeder cells [Fig. 4B]). The diffuse nature of the Cdyl signal in the H3K9me2-deficient cells suggested a delocalization of Cdyl from chromatin. Indeed, WB analysis of chromatin fractions confirmed that in the absence of H3K9me2, Cdyl's interaction with chromatin is reduced (Fig. 4C, top). In agreement, WB analysis of HS nuclear extracts, as well as IF assays, showed that Cdyl is still present in the nucleus but not in the chromatin fraction (Fig. 4B and C). The absence of Cdyl from the chromatin

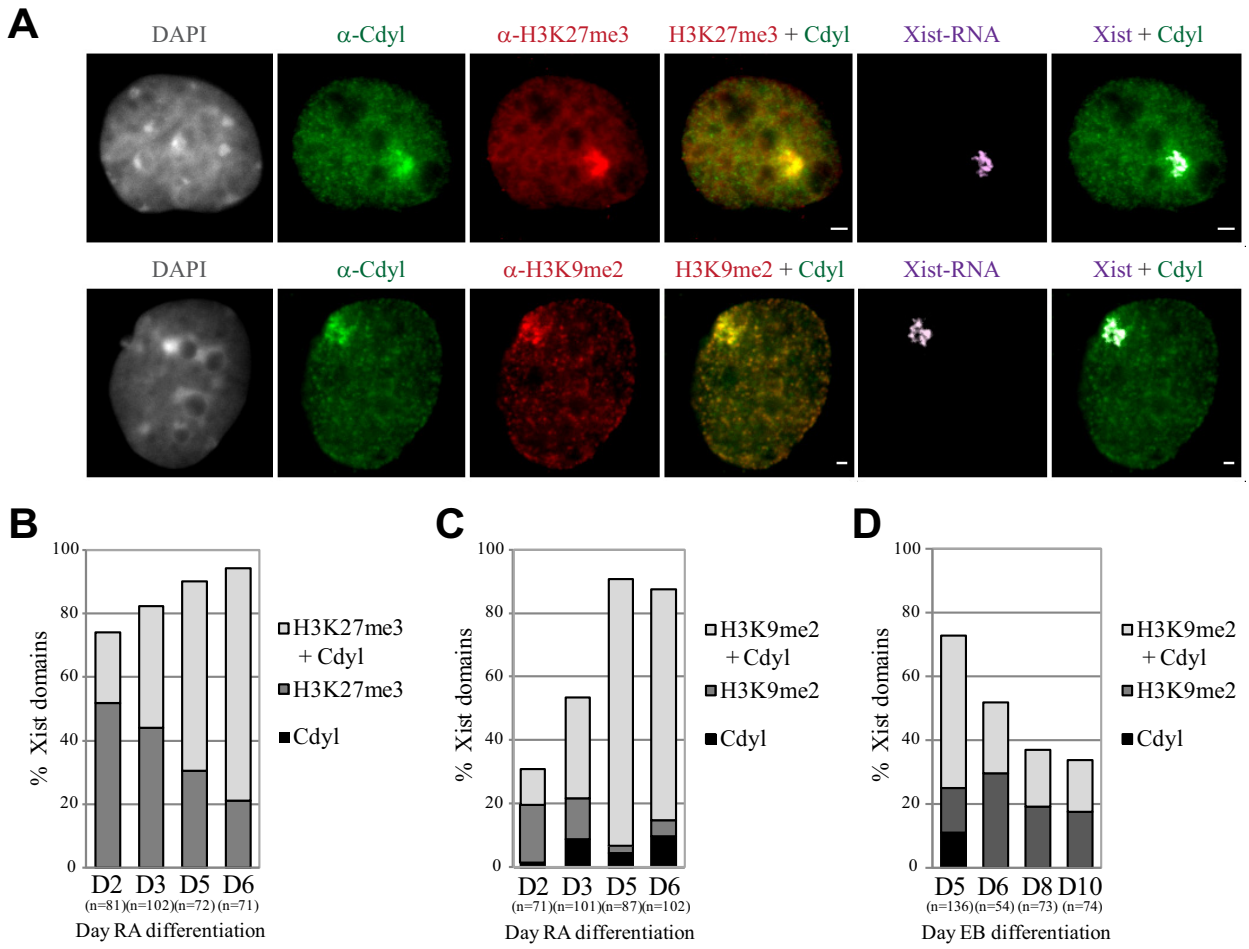

FIG 3 Cdyl recruitment to chromatin follows H3K27me3 and H3K9me2. mESCs at day 5 of RA differentiation are shown in panel A. The relative kinetics of incorporation of Cdyl into Xi in relation to those of H3K27me3 (B) and H3K9me2 (C and D) incorporation were determined by double IF assays with anti-Cdyl/anti-H3K27me3 or anti-Cdyl/anti-H3K9me2 antibody, combined with Xist RNA FISH. EB, embryoid bodies. The percentage of enrichment is shown in relation to the total number of Xist domains.

fraction could be explained by the absence of H3K9me2, or the G9a protein itself, as Cdyl and G9a have been proposed to interact (26, 46, 47). To explore this further, *G9a*$^{-/-}$ or WT mESCs were differentiated. In differentiated *G9a*$^{-/-}$ mutant ESCs, H3K9me2 levels were recovered partially based on WB and IF (Fig. 4B [bottom] and D), implying that an alternative HMT can lay down the H3K9me2 mark during differentiation. In differentiated *G9a*$^{-/-}$ cells, we also observed relocalization of Cdyl to chromatin on the basis of IF assays and WB analysis (Fig. 4B and D). The Cdyl relocalization did not quite reach the levels or distribution observed in differentiating WT cells (Fig. 4D), however, in agreement with only partial H3K9me2 recovery. We also noted a partial reduction of H3K9me3 levels in *G9a*$^{-/-}$ mutant ESCs (Fig. 4D and reference 48). Since Cdyl has also been found to interact with H3K9me3 by peptide pulldown (Fig. 1A) (20, 21), the effect on Cdyl's interaction with chromatin observed in *G9a* mutant cells could also be a consequence of this H3K9me3 reduction. However, we found that the recovery of Cdyl binding to chromatin upon differentiation seemed to follow closely the reincorporation of H3K9me2 in the time period analyzed here, whereas the H3K9me3 levels did not change compared to the undifferentiated state. Furthermore, Cdyl was never observed to be enriched at pericentric heterochromatin (chromocenters), which are highly enriched in H3K9me3. Thus, the general recruitment of Cdyl to chromatin appears to depend mainly on the presence of H3K9me2, rather than H3K9me3, or on the G9a protein.

In conclusion, our data suggest that H3K9me2 is a key chromatin mark for the general recruitment of Cdyl to chromatin. On the other hand, H3K27me3 is not required for general Cdyl chromatin association, although we do not rule out the possibility that it has a role in recruiting Cdyl to more specific regions of the genome.

A role for both the H3K27me3 and H3K9me2 histone marks in the recruitment of Cdyl to the Xist RNA-coated chromosome. Although H3K27me3 may not be globally required for Cdyl binding to chromatin, we explored whether it may nevertheless participate in the more specific targeting of Cdyl to Xi during XCI. For this, we used male ESCs containing an inducible autosomal *Xist* transgene on chromosome 11 (cell line 36:11). Both WT and *Eed*$^{-/-}$ mutant (16) *Xist*-inducible cells were available. We could thus examine whether Xist RNA can trigger Cdyl enrichment to a Xist RNA-coated chromosome in the presence or absence of

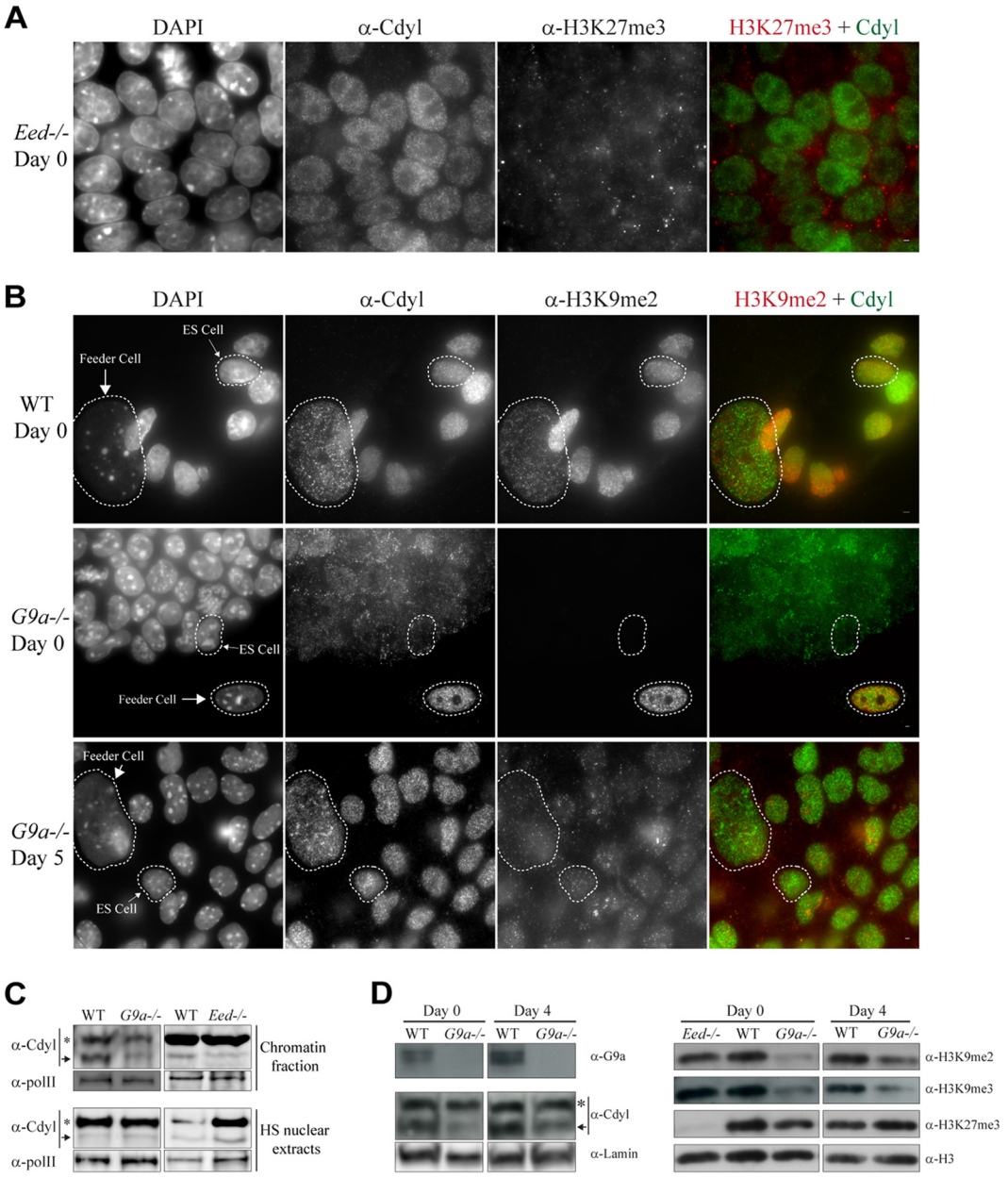

FIG 4 Cdyl recruitment to chromatin is dependent on H3K9me2. (A and B) The effect of the absence of H3K27me3 (A) or H3K9me2 (B) on the recruitment of Cdyl was determined by double IF assays in an *Eed* mutant ESC line (A) and a G9a HMT mutant ESC line (B) undifferentiated and after 5 days of RA differentiation. As both $G9a^{-/-}$ mutant mESCs and the parental TT2 cells grow on feeders, the presence of traces of (WT) feeder cells provided a control for positive H3K9me2/Cdyl staining. (C and D) WB analysis for Cdyl and histone posttranslational modifications in the same cell lines at day 0 (D0) and throughout RA differentiation. Anti-polymerase II (α-polII) or antilamin antibodies were used as loading controls. Each arrow shows the position of a Cdylb band, and each asterisk shows a nonspecific band.

H3K27me3 (16, 28). Importantly, previous work demonstrated that Xist RNA-mediated silencing steps are recapitulated in the WT transgenic mESC lines, including Xist RNA coating, gene silencing, and recruitment of heterochromatin marks such as H3K27me3 (18, 28, 29).

We first analyzed the degree of recruitment of Cdyl following doxycycline induction of *Xist* and retinoic acid (RA) differentiation of WT 36:11 cells. Using IF/RNA FISH, the H3K9me2 and H3K27me3 marks, as well as Cdyl, were observed on the Xist-coated chromosome with patterns comparable to those of WT female ESCs (Figs. 3B and 5A and B). In $Eed^{-/-}$ 36:11 cells, the overall H3K9me2 levels appeared unaffected (Fig. 5E) and general binding of Cdyl to chromatin was only mildly affected (Fig. 5E), as expected from our previous analysis (Fig. 4). Surprisingly, in the *Eed* mutant cells, no H3K27me3, H3K9me2, or Cdyl enrichment was detectable on the Xist RNA-coated chromosome following *Xist* induction (Fig. 5C and D). This implies that PRC2/H3K27me3 may be specifically required for the association of both H3K9me2 and Cdyl with the Xist RNA-coated chromosome. The absence of H3K9me2 enrichment on the Xist-coated chromo-

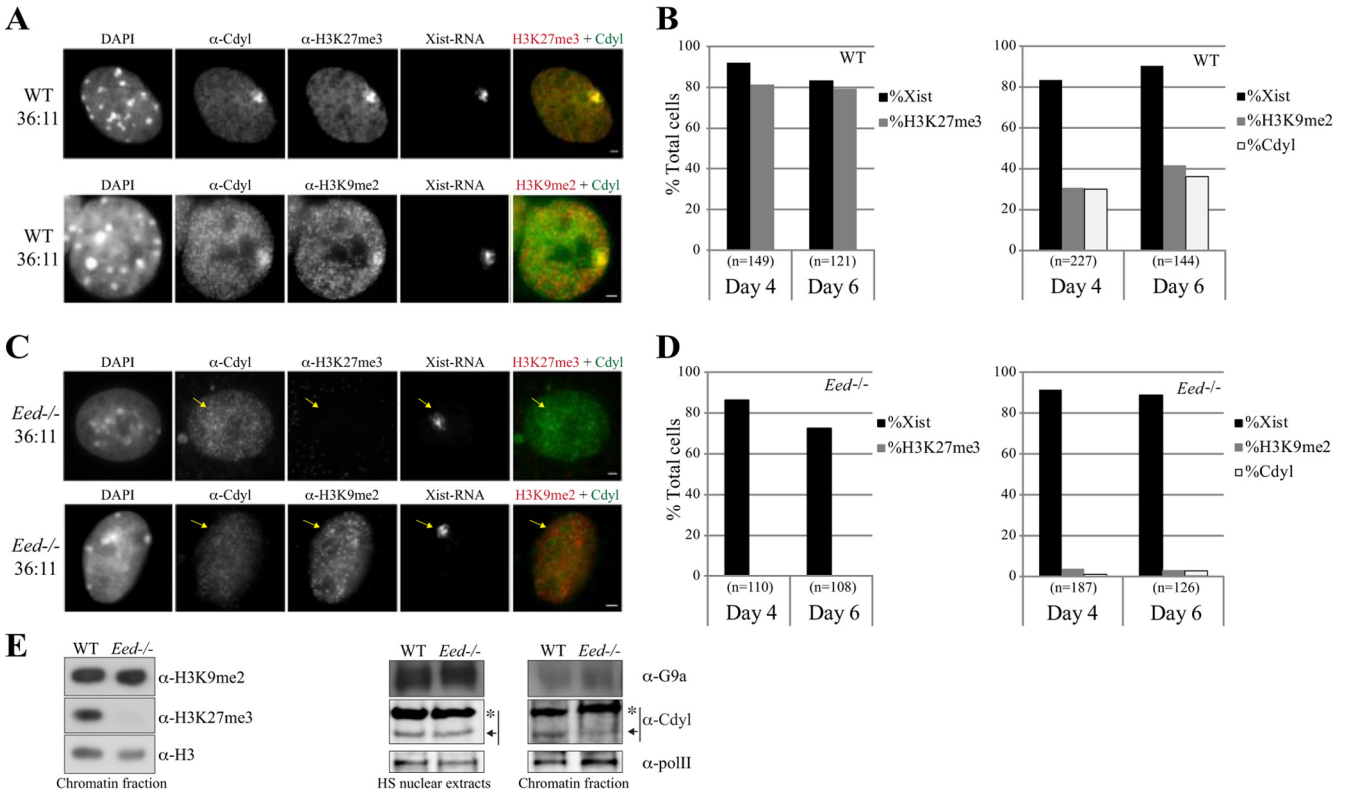

FIG 5 Cells lacking H3K27me3 fail to incorporate H3K9me2 and to recruit Cdyl to Xi. XY mESCs containing an inducible *Xist* transgene on chromosome 11 (36:11) (28) were used. (A and B) Double anti-Cdyl/anti-H3K27me3 and anti-Cdyl/anti-H3K9me2 assays combined with Xist RNA FISH show that after RA differentiation and Xist-doxycycline induction, the Xist RNA-coated chromosome recruits H3K27me3, H3K9me2, and Cdyl. (C and D) The same analysis was performed in a $Eed^{-/-}$ mutant background, where cells lack H3K27me3 (16). H3K9me2 incorporation and Cdyl recruitment were reduced in the absence of Eed. The arrows show the Xist-coated chromosome. (E) WB analysis of HS and chromatin fractions of the cell lines used in these experiments. Anti-H3 or anti-polymerase II (α-polII) antibodies were used as a loading control. Each arrow shows the position of a Cdylb band, and each asterisk represents a nonspecific band. Panels A and C show mESCs at day 6 of RA differentiation.

some in *Eed* mutant cells suggests that H3K27me3, or associated factors, may be required in order to lay down H3K9me2 efficiently on Xi. This, in turn, may affect Cdyl's enrichment with Xi.

Taken together, our results suggest that both H3K27me3 and H3K9me2 are required to recruit and/or maintain Cdyl levels at Xist RNA-coated chromatin and that a complex interplay exists between these two marks and the Cdyl protein on Xi.

The association of Cdyl with Xi is more stable than that of the PcG protein Cbx7. We next investigated the stability of Cdyl's association with Xi, compared to other factors, such as the PcG (PRC1) protein Cbx7, which also contains a chromodomain and was previously shown to interact with H3K27me3 (but not H3K9me2) and to associate with Xi (49). To this end, we performed FRAP of Cdyl-GFP- or Cbx7-GFP-expressing female ESCs differentiated for 3 to 5 days. We observed a strikingly slower recovery of fluorescence for Cdyl on Xi (Fig. 6A), compared to other regions of the nucleus, suggesting a rather low turnover and stable association with Xi. Cbx7-GFP, on the other hand, recovered faster than Cdyl-GFP and with the same kinetics on Xi compared to other regions (Fig. 6B). This suggests either that Cbx7 has a higher turnover and/or a lower affinity for Xist RNA-coated chromatin than Cdyl-GFP. Thus, although Cdyl seems to be present only transiently during the cell cycle, it appears to be rather stably associated with Xi, perhaps because of its interaction with both H3K27me3 and H3K9me2, which may result in slower recovery after FRAP than that of the PRC1 subunit Cbx7, which only binds to H3K27me3. Alternatively, Cdyl's slow recovery after FRAP may indicate a rate-limiting step in the formation of new Xist complexes and/or methylated histones that are competent to recruit new Cdyl.

Xist RNA coating and H3K27me3 are insufficient to recruit Cdyl; H3K9me2 and differentiation are also required. To evaluate further the requirements of Cdyl's association with Xi, we investigated whether Xist RNA coating triggered the recruitment of Cdyl prior to differentiation. We therefore induced *Xist* in undifferentiated 36:11 ESCs for 3 days. No Cdyl enrichment was observed to colocalize with the Xist-coated chromosome, unlike in differentiating 36:11 cells examined in parallel (Fig. 7A and B). We also noted a lack of H3K9me2 enrichment on the Xist-coated chromosome in undifferentiated ESCs (Fig. 7B), whereas H3K27me3 enrichment was detected at almost the same level in ESCs and in differentiating cells, as previously reported (18). Taken together, these observations demonstrate that Xist RNA coating and H3K27me3 are not sufficient for Cdyl recruitment and that differentiation is required for both H3K9me2 enrichment and Cdyl's association with the Xist-coated chromosome. It was previously proposed that differentiation may be required for condensation of Xist-coated chromatin (50). These results, together with our FRAP analyses (Fig. 6A and B), suggest that Cdyl and H3K9me2 occur in the

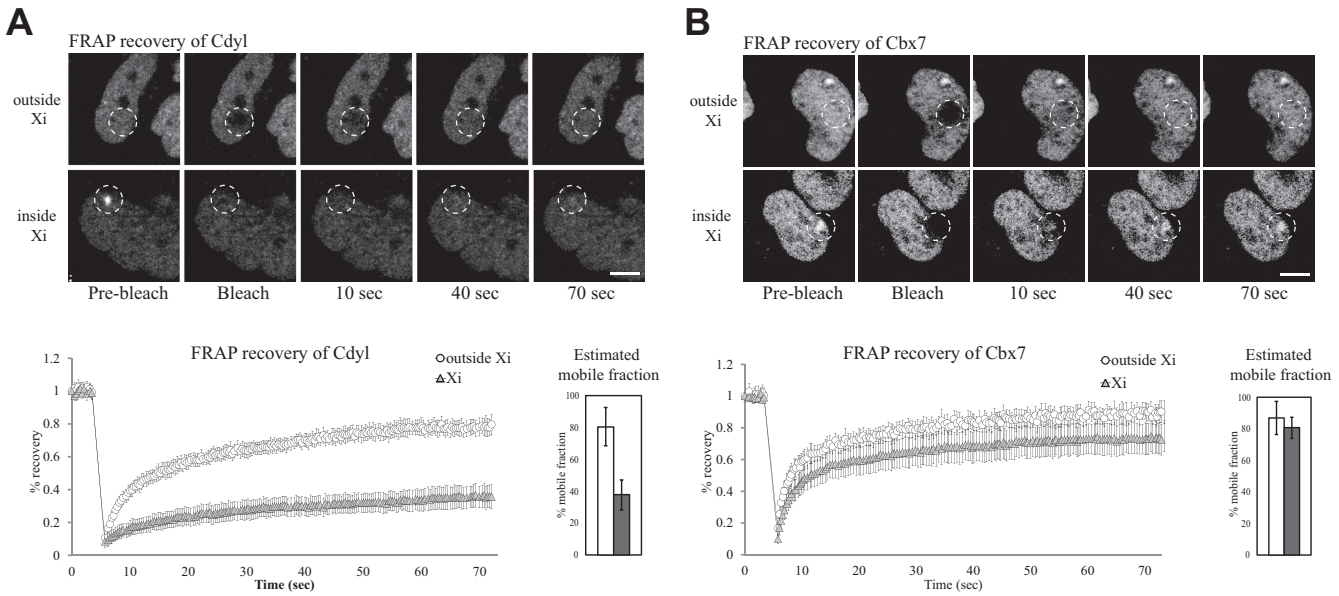

FIG 6 Cdyl dynamics are different inside or outside the *Xist* domain as measured by FRAP in differentiated ESCs. FRAP of Cdyl-GFP (A) or Cbx7-GFP (B) cell lines at day 4 of RA differentiation was performed in a region located either outside or inside the Xist RNA domain. Recovery kinetics were measured over a period of 1.26 min. Cdyl recovery outside the Xist domain was significantly faster than that within the Xist domain. No differences were found for Cbx7. The bar graphs represent the estimated mobile fractions. Values represent averages of at least 27 cells ± the standard deviations. The mean time for 50% Cdyl recovery in the Xist domain was 28.04 ± 9.97 s, and that outside the Xist domain was 7.28 ± 2.36 s. The mean time for 50% Cbx7 recovery in the *Xist* domain was 4.47 ± 0.96 s, and that outside the Xist domain was 4.47 ± 1.59 s. Cells were also recorded for 230 s (not shown) with consistent results.

context of Xi chromosome condensation and may even participate in facultative heterochromatin formation.

We next investigated the mechanisms underlying the maintenance of Cdyl on the Xist-coated chromosome during differentiation by removing doxycycline and *Xist* activation at different stages and examining the impact on Cdyl localization. We observed that removal of Xist RNA leads to rapid loss of Cdyl enrichment and H3K9me2 in differentiating ESCs, even though H3K27me3 can still be detected on the previously Xist-coated chromosome for at least 2 days (Fig. 7C). Thus, Xist RNA, or the factors it recruits (including PRC2), appear to have a role in maintaining Cdyl and H3K9me2 enrichment during differentiation.

In conclusion, our data show that Cdyl recruitment to the Xist-coated chromosome is a differentiation-dependent process and that the recruitment and maintenance of this protein require a combination of the H3K9me2 and H3K27me3 marks, as well as Xist RNA and/or its downstream changes.

Cdyl recruitment requires Xist RNA but not the Xist A-repeat region. Given the previously reported role of Cdyl in mediating transcriptional repression (25, 27), we asked whether it might play a role in Xist RNA-mediated silencing (29). We examined a mESC line with a doxycycline-inducible *Xist* gene with a mutated A-repeat region, which is essential for Xist's gene-silencing role (ΔSX cell line) (29) (Fig. 7D). This *Xist* mutant is still capable of coating the chromosome in *cis* but cannot induce transcriptional inactivation (29). Using IF/Xist RNA FISH following doxycycline XistΔA induction and RA-induced differentiation, we found that H3K9me2 and Cdyl were efficiently enriched on the XistΔA-coated chromosome, indicating that they do not play a role in the initiation of gene silencing (Fig. 7D). H3K27me3 enrichment was also normal, in agreement with previous results (18).

Cdyl is an essential protein during early ESC differentiation and interacts with MGA and G9a, which also associate with Xi. To investigate the role of Cdyl in the maintenance of XCI, we generated clonal mESC lines expressing short hairpin RNAs (shRNAs) directed against Cdyl (both Cdyla and Cdylb). Two different shRNAs targeting Cdyl were tested in parallel with control shRNAs on male and female ESCs (data not shown). These Cdyl-deficient ESCs showed a severely compromised capacity to differentiate, expressing higher levels of pluripotency markers and massive cell death (data not shown). In conclusion, Cdyl appears to be a vital protein during the early differentiation of both male and female cells. Its role in XCI could thus not be explored within the time window in which this process occurs and Cdyl presumably plays its role.

To gain further insight into the possible role that Cdyl might play in XCI and to explore the mechanism by which it is recruited to Xi, we decided to investigate the protein partners of Cdyl by using a label-free quantitative mass spectrometry approach (38). Female mESC cells stably expressing Cdyl-GFP at subendogenous levels were used (see Materials and Methods and Fig. 8A and B). Analysis of these transgenic mESC lines during differentiation revealed correct localization of the GFP-tagged Cdyl protein to the Xist RNA domain (Fig. 8A). Furthermore, the kinetics of Cdyl-GFP relative to H3K9me2 and H3K27me3 enrichment on Xi were similar to those in the parental cell line (data not shown). These Cdyl-GFP transgenic female ESCs were used, both undifferentiated and after 4 days of differentiation, to perform GFP affinity purifications of Cdyl. The summed intensity of all of the peptides of a protein (LFQ intensity) correlates with its abundance in a sample but does not indicate whether it is a specific binder or not. To distinguish between true Cdyl interactors and background proteins, two control experiments were performed. The first con-

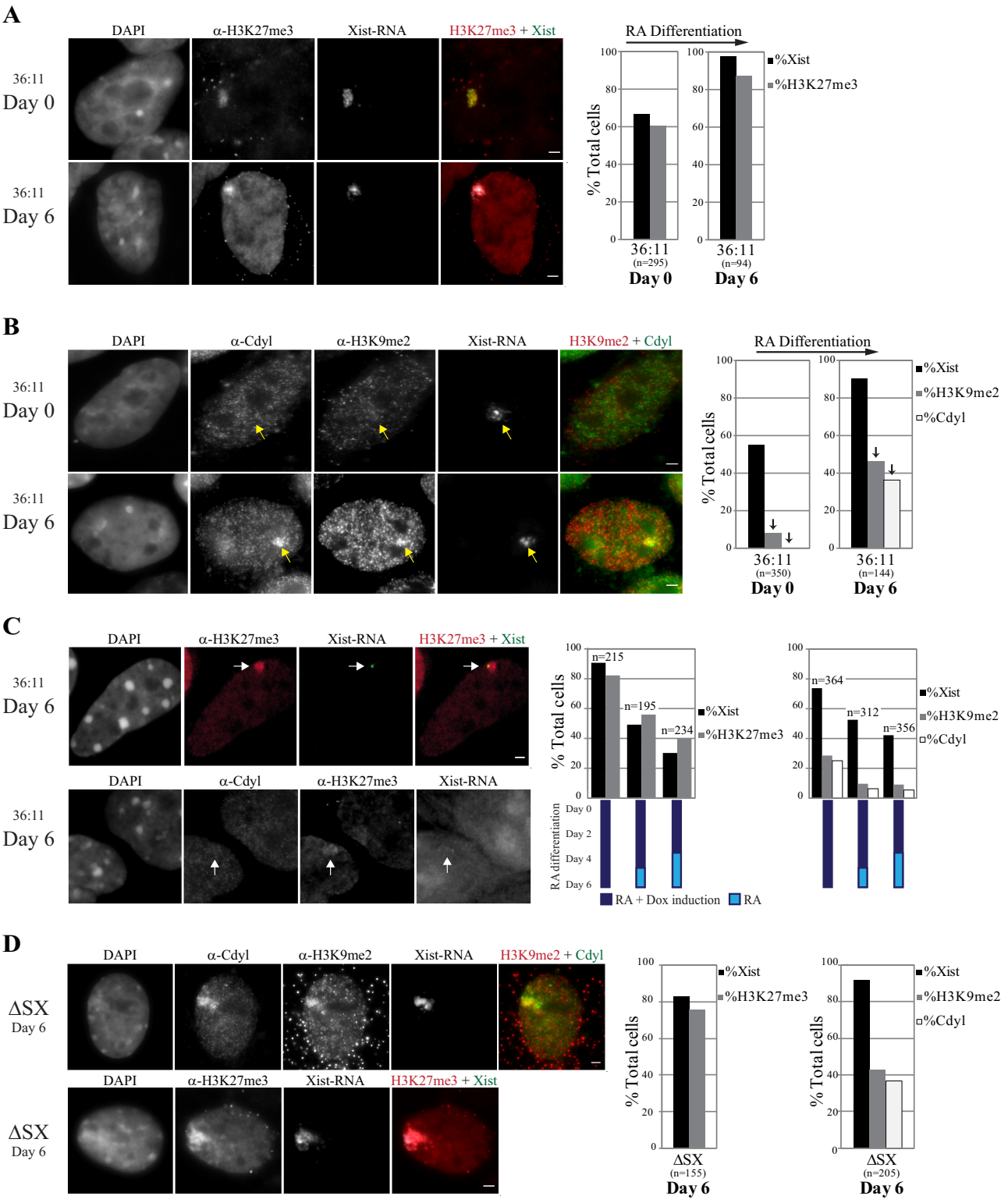

FIG 7 Cdyl recruitment depends on differentiation and is independent of the A-repeat region of Xist RNA. (A and B) IF assay-Xist RNA FISH experiments with undifferentiated and RA differentiated 36:11 cells induced for *Xist* expression with anti-H3K27me3 (A) or anti-H3K9me2 (B) antibodies show that high levels of H3K9me2 incorporation and Cdyl recruitment to the Xist RNA-coated domain are dependent on differentiation. 36:11 ESCs were doxycycline induced for 3 days in the presence of LIF or for 6 days in the presence of RA. (C) Xist RNA coating is essential for maintenance of Cdyl, H3K9me2, and H3K27me3 recruitment to the Xist-coated chromosome. Xist-inducible 36:11 mESCs were RA differentiated for 6 days. Doxycycline was either maintained for 6 days (dark blue bars) or washed out 2 or 3 days before the day of the experiment (light blue bars). Xist RNA FISH combined with anti-H3K27me3 IF assay or double IF assay for anti-Cdyl/anti-H3K9me2 was performed. White arrows show enrichment/absence of the mark/protein in the Xist-coated chromosome. (D) IF assay-Xist RNA FISH analysis of Xist ΔA-repeat region mutant (ΔSX) ESCs reveals that the A-repeat region of Xist is not required to recruit H3K27me3, Cdyl, or H3K9me2. Yellow arrows indicate the Xist RNA-coated chromosome.

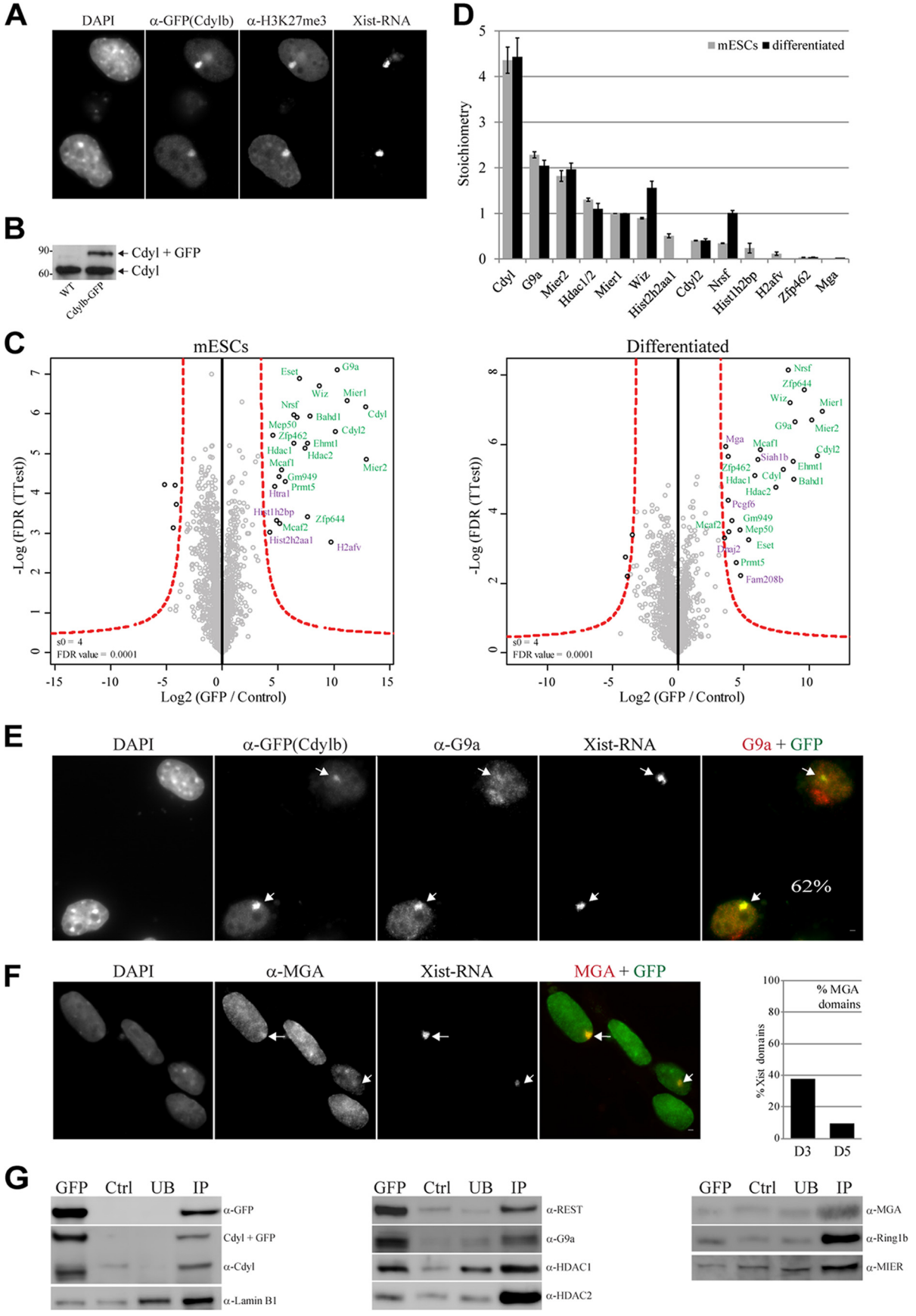
A
DAPI
α-GFP(Cdylb)
α-H3K27me3
Xist-RNA
B
90-
60-
Cdyl + GFP
Cdyl
WT
Cdylb-GFP
C
mESCs
Differentiated
-Log (FDR (TTest))
Log2 (GFP / Control)
s0 = 4
FDR value = 0.0001
Eset
G9a
Wiz
Mier1
Nrsf
Cdyl
Bahd1
Mep50
Cdyl2
Zfp462
Ehmt1
Hdac1
Hdac2
Mier2
Mcaf1
Gm949
Prmt5
Htra1
Hist1h2bp
Zfp644
Mcaf2
Hist2h2aa1
H2afv
Zfp644
Mga
Siah1b
Pcgf6
Dnaj2
Fam208b
D
mESCs
differentiated
Stoichiometry
Cdyl
G9a
Mier2
Hdac1/2
Mier1
Wiz
Hist2h2aa1
Cdyl2
Nrsf
Hist1h2bp
H2afv
Zfp462
Mga
E
DAPI
α-GFP(Cdylb)
α-G9a
Xist-RNA
G9a + GFP
62%
F
DAPI
α-MGA
Xist-RNA
MGA + GFP
% MGA domains
% Xist domains
D3
D5
G
GFP
Ctrl
UB
IP
α-GFP
Cdyl + GFP
α-Cdyl
α-Lamin B1
α-REST
α-G9a
α-HDAC1
α-HDAC2
α-MGA
α-Ring1b
α-MIER

sisted of affinity purification with the same beads in nuclear extract from WT cells; the second consisted of affinity purification with control beads lacking GFP affinity in the same GFP-Cdyl-rich nuclear extract. The two controls gave similar results (data not shown). Each purification was performed in triplicate, and proteins with significantly higher LFQ values in the GFP-Cdyl purification than in the control purifications are specific binders, as indicated to the right of the volcano plots in Fig. 8C.

We identified over 20 proteins that were significantly associated with Cdyl (Fig. 8C) before and after differentiation. Many of the copurified proteins have previously been reported to interact with Cdyl, validating our approach. These include histone deacetylase 1 (HDAC1) and HDAC2 (25), the neuron-restrictive silencer factor (NRSF also known as REST), and the G9a HMT (26). The purifications also revealed an interaction between Cdyl and the mesoderm induction early response 1 (MI-ER1) protein, a transcriptional corepressor that binds HDAC1 (51), and its homolog MI-ER2, as well as two large multi-zinc finger proteins, ZNF462 and ZNF644. A group of proteins, including the MAX gene-associated (MGA) protein, was of particular interest with respect to XCI because this group only interacted with Cdyl in differentiating ESCs and might therefore be linked to the differentiation-dependent association of Cdyl with Xi. From this group, MGA and G9a had previously been shown to belong to the E2F6 complex that has been proposed to provide an alternative mechanism for Ring1B recruitment and H2A monoubiquitylation of Xi (52).

We also quantified the stoichiometry of the interactors by using a label-free relative quantification approach (53). Stoichiometry analysis (Fig. 8D) revealed several core Cdyl interactors, including Wiz and Nrsf (also known as REST) which, interestingly, show an increase in their stoichiometry relative to Cdyl during differentiation. Some of the observed interactions were confirmed by chromatin immunoprecipitation (IP) with Cdyl-GFP ESCs (Fig. 8G). We also noted that the endogenous Cdyl protein was pulled down in IPs with Cdyl-GFP, confirming previous reports that the mouse Cdyl protein can multimerize (21). This observation is also in agreement with our stoichiometry determination. The Cdyl2 protein, also identified as an interactor of Cdyl, was found to be present at very low stoichiometric levels (about 10% relative to Cdyl itself). Cdyl also immunoprecipitated with the REST and G9a proteins and more weakly with HDAC1 and HDAC2. Although the MGA and Mier proteins were not found to interact with Cdyl by IP, this may be due to the poor quality of the antibodies available in both cases or reflect the low stoichiometry that these proteins exhibit in relation to Cdyl (Fig. 8D). We also investigated the association of the above-mentioned proteins on Xi by using IF assays combined with Xist RNA FISH. Only some of these antibodies showed satisfactory staining in IF assays. We found that the HDAC1, HDAC2, and REST proteins were present on Xi but not particularly enriched (unpublished observations). On the other hand, the MGA and G9a proteins clearly colocalized with Xi, though only in a proportion of the cells (Fig. 8E and F). Further analysis of MGA localization at days 3 and 5 of differentiation in Cdyl-GFP mESCs, as well as in XEN cells, revealed that MGA associates with Xi within the same time window as Cdyl (Fig. 8F and data not shown). In the case of G9a, a small proportion of the cells showed an association with Xi both in differentiating mESCs and in XEN cells (Fig. 8E and data not shown). To assess the enrichment of G9a relative to Cdyl on Xi, the Cdyl-GFP cell line was analyzed by using Xist RNA FISH combined with anti-GFP/anti-G9a IF assays (Fig. 8E). G9a was found enriched on Xi only in cells with Cdyl-GFP Xi enrichment, i.e., in 62% of the Cdyl-positive Xist RNA domains (13% of the total cells, $n = 80$).

In conclusion, we show that Cdyl interacts with a variety of proteins, including itself, as well as the MGA and G9a proteins. This suggests that G9a may be one of the HMTs involved in the deposition of H3K9me2 on Xi and that Cdyl may participate in the recruitment of these and other proteins to Xi.

DISCUSSION

The chromatin changes that take place during XCI and the formation of facultative heterochromatin may provide important insights into our understanding of the mechanisms by which silencing occurs and is maintained. In this study, we uncovered Cdyl as a novel protein partner of Xi and a "reader" of H3 histone marks on this chromosome. Cdyl is transiently recruited to the X chromosome undergoing inactivation during early mESC differentiation. Previous reports have shown that Cdyl can act as a transcriptional corepressor (25) and participate in gene silencing (27). In the present study, we found that initiation of X inactivation occurs in the absence of Cdyl association. Thus, the likely role of Cdyl in XCI is not in the establishment of gene silencing but rather in the maintenance of the inactive state, possibly through the particular chromatin structure that it recognizes and participates in stabilizing.

Cdyl's interaction with the chromatin of Xi *in vivo* depends on H3K9me2, H3K27me3, and Xist RNA. Previous studies have shown that Cdyl can interact with various histone marks, including H3K9me2, H3K9me3, and H3K27me3 (20, 21, 54). Cdyl has also been reported to interact with the G9a protein, as confirmed here. Our study reveals that *in vivo*, H3K9me2 is required for Cdyl's interaction with chromatin, as in the absence of the H3K9me2 HMT, G9a, the Cdyl protein is released from chromatin, as shown by IF assays and WB analysis. Importantly, we also show that it is the H3K9me2 mark, rather than G9a *per se*, that

FIG 8 MGA and G9a interact with Cdyl and are recruited to Xi. (A) IF assay-FISH of a Cdyl-GFP female ESC line shows GFP-Cdyl recruitment to Xi with an anti-GFP antibody combined with Xist RNA FISH. (B) WB of chromatin fractions with anti-GFP antibody on day 5 of RA differentiation. The values to the left are molecular sizes in kilodaltons. (C) Volcano plots from mass spectrometry data generated by anti-GFP antibody immunoprecipitation from nuclear extracts of the GFP-Cdyl cell line at undifferentiated and differentiated stages. The LFQ ratio of the Cdyl to the control purification is plotted on the *x* axis, and the *P* value of the *t* test is plotted on the *y* axis. The proteins indicated on the right side outside the red line are significantly enriched (permutation-based FDR with $P = 0.0001$ and $S0 = 4$) in the Cdyl purification and are thus specific interactors. Proteins highlighted in purple correspond to those found in only one of the mESC differentiation states. (D) Stoichiometry of chromatin-associated protein complexes, determined as previously reported (53), shows Cdyl interactors. (E and F) Two interactors, MGA and G9a, are recruited to Xi. (E) Double IF assay-Xist RNA FISH of the GFP-Cdyl cell line at day 3 of RA differentiation showing recruitment of G9a to Xi. The percentage of cells with G9a enrichment is shown in relation to number of Cdyl-GFP-positive signals on Xi. (F) IF assay-FISH of mESCs with an anti-MGA antibody shows MGA staining on Xi (arrows). Quantification of cells showing MGA incorporation in Xist domains. (G) WB analysis of anti-GFP antibody immunoprecipitation from nuclear extracts of the GFP-Cdyl cell line differentiated with RA to day 4. Ctrl, control; UB, unbound.

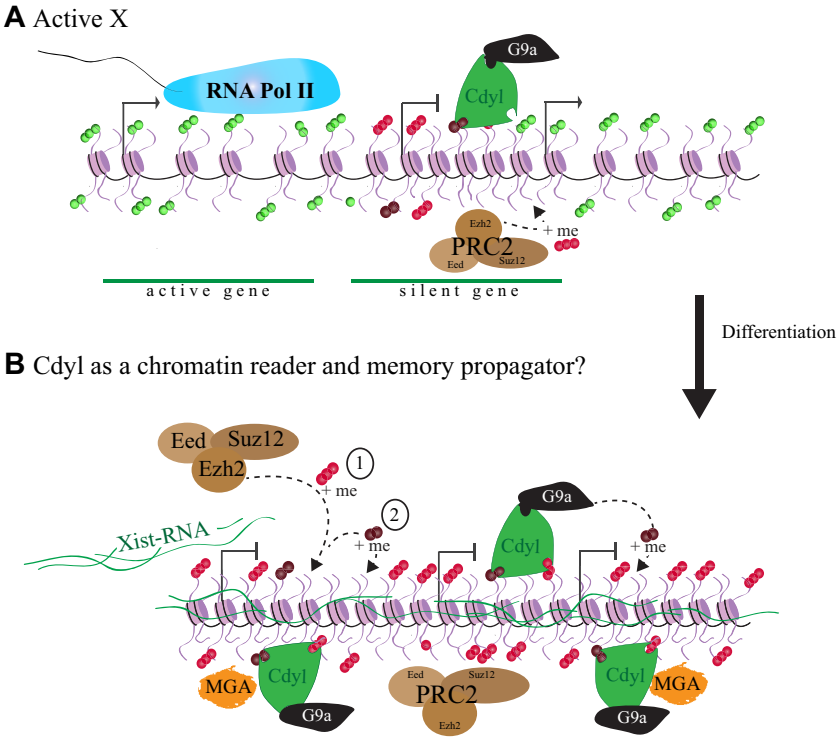

FIG 9 Model of Cdyl in the process of XCI. (A) The active X chromosome. (B) In mESCs after differentiation has begun, Xist RNA accumulation (green lines) on Xi is followed by PRC2 recruitment and H3K27 methylation (red circles), as well as an accumulation of H3K9me2 (brown circles). We propose a hierarchical order of the incorporation of these two marks. These combinations of marks, cell differentiation, and chromatin condensation may facilitate Cdyl (green protein) stabilization to specific genomic regions, including Xi. Cdyl's interaction with chromatin is likely to facilitate the recruitment of other proteins to Xi, including the H3K9me2 HMT G9a, supporting a feedforward mechanism of H3K9me2 propagation. Cdyl could participate as part of the machinery that ensures the propagation of the inactive state through part, but not all, of the cell cycle (Fig. 1D). On the basis of IP experiments and a previous report (21), the mouse Cdyl protein may interact as a trimer.

influences Cdyl recruitment to chromatin in differentiating ESCs. In the context of XCI, we show that the H3K27me3 modification appears to be important for Cdyl's association with the Xist RNA-coated chromosome in differentiating ESCs. Lack of this mark (in *Eed* mutant cells) results in a reduction of both Cdyl and H3K9me2 enrichment on the Xist-coated chromosome. Cdyl was never seen without H3K9me2 enrichment in this context, supporting the idea that its recruitment is linked to the H3K9me2 mark. The requirement of PRC2/H3K27me3 for Cdyl recruitment to the Xist-coated chromosome may be an indirect effect of the dependence of H3K9me2 enrichment on H3K27me3 that we have uncovered here. Indeed, H3K9 methylation via G9a/GLP was recently proposed to depend on the presence of H3K27 methylation (55), with the mutation of lysine 27 to alanine impairing H3K9 dimethylation via G9a. Our results suggest a similar interplay between the H3K9me2 and H3K27me3 marks, as well as the Cdyl protein, on Xi. The presence of both H3K9me2 and H3K27me3 may provide a signature that increases the overall binding of Cdyl to Xi, as supported by our peptide pulldowns on a Cdyl-GFP cell line and FRAP analysis, and this enables the subsequent anchoring of the G9a/Cdyl complex to H3K9me2/H3K27me3-marked Xi. The fact that Cdyl closely follows H3K9me2 and H3K27me3 kinetics on Xi, even though Cdyl mRNA and protein levels do not change significantly during early differentiation, provides additional evidence that it is the presence of these two marks that somehow dictates its appearance on Xi. Furthermore, we have shown that in undifferentiated ESCs, where Xist RNA coating induces only low levels of H3K9me2 incorporation (10-fold lower than those in differentiated cells) and high levels of H3K27me3, this is not sufficient for Cdyl recruitment. Thus, additional factors/chromatin features present only during differentiation must be required for the recruitment of both H3K9me2 and Cdyl to the Xist-coated chromosome.

Putative role of Cdyl as a chromatin reader and memory propagator in X inactivation. The function of Cdyl in XCI remains elusive, as it appears to be an essential protein for cell viability and differentiation on the basis of the massive cell death we observed during the differentiation of ESCs with Cdyl knocked down. A recent study with Cdyl knockout mice suggested that Cdyl has a role in neuronal differentiation (56), although the precise nature of the mutated allele used was not described. Nevertheless, Cdyl, H3K9me2, and H3K27me3 become enriched on the Xist RNA-coated chromosome in the absence of gene silencing, implying that neither Cdyl nor the two histone modifications are sufficient to trigger transcriptional repression. This is also consistent with previous findings showing that in *Eed* mutant cells, Xist RNA coating and initiation of gene silencing occur normally (16). Taken together, these findings imply that neither Cdyl nor

H3K9me2 or H3K27me3 is required for initiation of X inactivation (i.e., for Xist RNA coating or gene silencing), although it may be required for maintenance of the inactive state.

Investigation of the protein partners of Cdyl that we describe here should shed light on the possible mechanisms that participate in Cdyl's recruitment to Xi and its role there. In addition to G9a, we have identified the MAX gene-associated protein MGA, which was recently described as a member of an alternative PRC1 complex (named PRC1.6), with a possible role in Ring1B/Rnf2 targeting and H2A monoubiquitylation, that binds independently of H3K27me3 (52). Although stoichiometric analysis of mass spectrometry data suggests that MGA is not a major interactor of Cdyl, we find that it is recruited to Xi within the same time window as Cdyl. This suggests a potential new link between PRC1 and Xi. In a recent study, Tavares et al. showed that different PRC1 complexes are targeted to Xi in both H3K27me3-dependent and -independent ways (via Cbx7 and RBYP, respectively) (17). Cdyl may provide another facet of PRC1's association with Xi. Finally, we also find that the Wiz and REST proteins show increased Cdyl interaction during differentiation and confirm that REST is a major interactor of Cdyl, although we did not find it to be particularly enriched on Xi by IF assay.

Putative role of Cdyl in self-templating maintenance on Xi. Our study has revealed that recruitment of Cdyl to chromatin seems to be largely dependent on the presence of H3K9me2, while recruitment to Xi may be dependent on the cooccurrence of H3K9me2 and H3K27me3. These two marks may stabilize Cdyl's interaction on Xi. Cdyl recruitment to Xi may, in turn, facilitate the recruitment of other proteins, including G9a. The fact that Cdyl seems to be cell cycle regulated, being enriched on Xi in G_1/S phase, whereas the PRC2 complex and the H3K27me3 mark are thought to be associated with Xi throughout the cell cycle during early differentiation, suggests that Cdyl cannot represent a mitotic memory mark on Xi. However, it may facilitate the perpetuation of H3K9me2, for example, during S phase, when histone modifications can be lost and must be restored. Cdyl may therefore participate in a memory loop, whereby it binds H3K9me2 (and H3K27me3) on Xi and at the same time helps to bring in the G9a HMT that may facilitate the maintenance of the H3K9me2 mark during the cell cycle. Thus, Cdyl may be part of a self-templating process that participates in the maintenance of facultative heterochromatin during the cell cycle.

Our current view of the processes underlying Cdyl's recruitment to Xi is summarized in the model shown in Fig. 9. We provide new insight into the hierarchy of chromatin modifications triggered by Xist RNA during XCI. Cdyl requires both H3K27me3 and H3K9me2 for chromatin association with the Xist-coated chromosome, while interacting with an H3K9me2 HMT. Cdyl may thus represent a potential reader of a "histone code," as postulated by Strahl and Allis (57) and Turner (58), in this case of Xi. The fact that Cdyl also interacts with G9a raises the exciting possibility that the "reader" can help bring in a "writer" of H3K9me2. This provides one of the first glimpses into the possible role of the unique combination of histone modifications of Xi and their participation in the recruitment of specific factors that may be involved in the perpetuation of the silent state.

ACKNOWLEDGMENTS

We thank members of the Heard lab, in particular, E. Nora and R. Duffié, for helpful advice and discussions, C. Picard for early experiments with Cdyl, and A.-V. Gendrel for critical input on Western blot analysis. We thank A. Wutz for Xist-inducible ESCs and S. Khochbin for Cdyl constructs and critical feedback.

M.E.-D.-A. was supported by an FRM fellowship. This work was supported by Ligue contre le Cancer, the ANR, the EpiGeneSys FP7 257082 Network of Excellence, ERC Advanced Investigator award 250367, and EU FP7 SYBOSS grant 242129 (E.H.). The Vermeulen lab is supported by a grant from the Netherlands Organization for Scientific Research (NWO-VIDI; project no. 864.09.003).

Contributions were as follows: biochemical and microscopy experiments, M.E.-D.-A. and S.T.D.R.; cell culture, M.E.-D.-A.; generation of plasmids and cell lines, M.E.-D.-A.; mass spectrometry, C.G.S., A.H.S., and M.V.; FRAP, O.R. and M.E.-D.-A.; experimental design, interpretation, and writing, E.H., M.E.-D.-A., M.V., and M.R.

We have no conflict of interest to declare.

REFERENCES

1. **Lyon MF.** 1961. Gene action in the X-chromosome of the mouse (Mus musculus L.). Nature **190:**372–373.
2. **Escamilla-Del-Arenal M, da Rocha ST, Heard E.** 2011. Evolutionary diversity and developmental regulation of X-chromosome inactivation. Hum. Genet. **130:**307–327.
3. **Heard E, Rougeulle C, Arnaud D, Avner P, Allis CD, Spector DL.** 2001. Methylation of histone H3 at Lys-9 is an early mark on the X chromosome during X inactivation. Cell **107:**727–738.
4. **Chaumeil J, Okamoto I, Guggiari M, Heard E.** 2002. Integrated kinetics of X chromosome inactivation in differentiating embryonic stem cells. Cytogenet. Genome Res. **99:**75–84.
5. **Okamoto I, Otte AP, Allis CD, Reinberg D, Heard E.** 2004. Epigenetic dynamics of imprinted X inactivation during early mouse development. Science **303:**644–649.
6. **Chaumeil J, Le Baccon P, Wutz A, Heard E.** 2006. A novel role for Xist RNA in the formation of a repressive nuclear compartment into which genes are recruited when silenced. Genes Dev. **20:**2223–2237.
7. **Csankovszki G, Nagy A, Jaenisch R.** 2001. Synergism of Xist RNA, DNA methylation, and histone hypoacetylation in maintaining X chromosome inactivation. J. Cell Biol. **153:**773–784.
8. **Mak W, Baxter J, Silva J, Newall AE, Otte AP, Brockdorff N.** 2002. Mitotically stable association of polycomb group proteins Eed and Enx1 with the inactive X chromosome in trophoblast stem cells. Curr. Biol. **12:**1016–1020.
9. **Silva J, Mak W, Zvetkova I, Appanah R, Nesterova TB, Webster Z, Peters AH, Jenuwein T, Otte AP, Brockdorff N.** 2003. Establishment of histone h3 methylation on the inactive X chromosome requires transient recruitment of Eed-Enx1 polycomb group complexes. Dev. Cell **4:**481–495.
10. **Plath K, Fang J, Mlynarczyk-Evans SK, Cao R, Worringer KA, Wang H, de la Cruz CC, Otte AP, Panning B, Zhang Y.** 2003. Role of histone H3 lysine 27 methylation in X inactivation. Science **300:**131–135.
11. **de Napoles M, Mermoud JE, Wakao R, Tang YA, Endoh M, Appanah R, Nesterova TB, Silva J, Otte AP, Vidal M, Koseki H, Brockdorff N.** 2004. Polycomb group proteins Ring1A/B link ubiquitylation of histone H2A to heritable gene silencing and X inactivation. Dev. Cell **7:**663–676.
12. **Fang J, Chen T, Chadwick B, Li E, Zhang Y.** 2004. Ring1b-mediated H2A ubiquitination associates with inactive X chromosomes and is involved in initiation of X inactivation. J. Biol. Chem. **279:**52812–52815.
13. **Zhao J, Sun BK, Erwin JA, Song JJ, Lee JT.** 2008. Polycomb proteins targeted by a short repeat RNA to the mouse X chromosome. Science **322:**750–756.
14. **Masui O, Heard E.** 2006. RNA and protein actors in X-chromosome inactivation. Cold Spring Harbor Symp. Quant. Biol. **71:**419–428.
15. **Cao R, Wang L, Wang H, Xia L, Erdjument-Bromage H, Tempst P, Jones RS, Zhang Y.** 2002. Role of histone H3 lysine 27 methylation in Polycomb-group silencing. Science **298:**1039–1043.
16. **Schoeftner S, Sengupta AK, Kubicek S, Mechtler K, Spahn L, Koseki H, Jenuwein J, Wutz A.** 2006. Recruitment of PRC1 function at the initiation of X inactivation independent of PRC2 and silencing. EMBO J. **25:**3110–3122.
17. **Tavares L, Dimitrova E, Oxley ED, Webster J, Poot R, Demmers J, Bezstarosti K, Taylor S, Ura H, Koide H, Wutz A, Vidal M, Elderkin S, Brockdorff N.** 2012. RYBP-PRC1 complexes mediate H2A ubiquitylation

at polycomb target sites independently of PRC2 and H3K27me3. Cell **148:**664–678.
18. **Kohlmaier A, Savarese F, Lachner M, Martens J, Jenuwein T, Wutz A.** 2004. A chromosomal memory triggered by Xist regulates histone methylation in X inactivation. PLoS Biol. **2:**E171. doi:10.1371/journal.pbio.0020171.
19. **Oda H, Okamoto I, Murphy N, Chu J, Price SM, Shen MM, Torres-Padilla ME, Heard E, Reinberg D.** 2009. Monomethylation of histone H4-lysine 20 is involved in chromosome structure and stability and is essential for mouse development. Mol. Cell. Biol. **29:**2278–2295.
20. **Vermeulen M, Eberl HC, Matarese F, Marks FH, Denissov S, Butter F, Lee KK, Olsen JV, Hyman AA, Stunnenberg HG, Mann M.** 2010. Quantitative interaction proteomics and genome-wide profiling of epigenetic histone marks and their readers. Cell **142:**967–980.
21. **Franz H, Mosch K, Soeroes S, Urlaub H, Fischle W.** 2009. Multimerization and H3K9me3 binding are required for CDYL1b heterochromatin association. J. Biol. Chem. **284:**35049–35059.
22. **Bartke T, Vermeulen M, Xhemalce B, Robson SC, Mann M, Kouzarides T.** 2010. Nucleosome-interacting proteins regulated by DNA and histone methylation. Cell **143:**470–484.
23. **Lahn BT, Page DC.** 1999. Retroposition of autosomal mRNA yielded testis-specific gene family on human Y chromosome. Nat. Genet. **21:**429–433.
24. **Dorus S, Gilbert SL, Forster ML, Barndt RJ, Lahn BT.** 2003. The CDY-related gene family: coordinated evolution in copy number, expression profile and protein sequence. Hum. Mol. Genet. **12:**1643–1650.
25. **Caron C, Pivot-Pajot C, van Grunsven LA, Col E, Lestrat C, Rousseaux S, Khochbin S.** 2003. Cdyl: a new transcriptional co-repressor. EMBO Rep. **4:**877–882.
26. **Mulligan P, Westbrook TF, Ottinger M, Pavlova N, Chang B, Macia E, Shi YJ, Barretina J, Liu J, Howley PM, Elledge SJ, Shi Y.** 2008. CDYL bridges REST and histone methyltransferases for gene repression and suppression of cellular transformation. Mol. Cell **32:**718–726.
27. **Zhang Y, Yang X, Gui B, Xie G, Zhang D, Shang Y, Liang J.** 2011. Corepressor protein CDYL functions as a molecular bridge between polycomb repressor complex 2 and repressive chromatin mark trimethylated histone lysine 27. J. Biol. Chem. **286:**42414–42425.
28. **Wutz A, Jaenisch R.** 2000. A shift from reversible to irreversible X inactivation is triggered during ES cell differentiation. Mol. Cell **5:**695–705.
29. **Wutz A, Rasmussen TP, Jaenisch R.** 2002. Chromosomal silencing and localization are mediated by different domains of Xist RNA. Nat. Genet. **30:**167–174.
30. **Tachibana M, Sugimoto K, Nozaki M, Ueda J, Ohta T, Ohki M, Fukuda M, Takeda N, Niida H, Kato H, Shinkai Y.** 2002. G9a histone methyltransferase plays a dominant role in euchromatic histone H3 lysine 9 methylation and is essential for early embryogenesis. Genes Dev. **16:**1779–1791.
31. **Montgomery ND, Yee D, Chen A, Kalantry S, Chamberlain SJ, Otte AP, Magnuson T.** 2005. The murine polycomb group protein Eed is required for global histone H3 lysine-27 methylation. Curr. Biol. **15:**942–947.
32. **Chaumeil J, Augui S, Chow JC, Heard E.** 2008. Combined immunofluorescence, RNA fluorescent in situ hybridization, and DNA fluorescent in situ hybridization to study chromatin changes, transcriptional activity, nuclear organization, and X-chromosome inactivation. Methods Mol. Biol. **463:**297–308.
33. **Rougeulle C, Chaumeil J, Sarma K, Allis CD, Reinberg D, Avner P, Heard E.** 2004. Differential histone H3 Lys-9 and Lys-27 methylation profiles on the X chromosome. Mol. Cell. Biol. **24:**5475–5784.
34. **Hamer KM, Sewalt RG, den Blaauwen JL, Hendrix T, Satijn DP, Otte AP.** 2002. A panel of monoclonal antibodies against human polycomb group proteins. Hybrid Hybridomics. **21:**245–252.
35. **Kuzmichev A, Jenuwein T, Tempst P, Reinberg D.** 2004. Different EZH2-containing complexes target methylation of histone H1 or nucleosomal histone H3. Mol. Cell **14:**183–193.
36. **Dignam JD, Lebovitz RM, Roeder RG.** 1983. Accurate transcription initiation by RNA polymerase II in a soluble extract from isolated mammalian nuclei. Nucleic Acids Res. **11:**1475–1489.
37. **Smith BA, Shelton DN, Kieffer C, Milash B, Usary J, Perou CM, Bernard PS, Welm BE.** 2012. Targeting the PyMT oncogene to diverse mammary cell populations enhances tumor heterogeneity and generates rare breast cancer subtypes. Genes Cancer **3**(9–10)**:**550–563.
38. **Hubner NC, Mann M.** 2011. Extracting gene function from protein-protein interactions using Quantitative BAC InteraCtomics (QUBIC). Methods **53:**453–459.
39. **Rappsilber J, Ishihama Y, Mann M.** 2003. Stop and go extraction tips for matrix-assisted laser desorption/ionization, nanoelectrospray, and LC/MS sample pretreatment in proteomics.. Anal. Chem. **75:**663–670.
40. **Fischle W, Wang Y, Allis CD.** 2003. Binary switches and modification cassettes in histone biology and beyond. Nature **425:**475–479.
41. **Mateescu B, England P, Halgand F, Yaniv M, Muchardt C.** 2004. Tethering of HP1 proteins to chromatin is relieved by phosphoacetylation of histone H3. EMBO Rep. **5:**490–496.
42. **Olsen JV, Vermeulen M, Santamaria A, Kumar C, Miller ML, Jensen LJ, Gnad F, Cox J, Jensen TS, Nigg EA, Brunak S, Mann M.** 2010. Quantitative phosphoproteomics reveals widespread full phosphorylation site occupancy during mitosis. Sci. Signal. **3:**ra3. doi:10.1126/scisignal.2000475.
43. **Mermoud JE, Popova B, Peters AH, Jenuwein T, Brockdorff N.** 2002. Histone H3 lysine 9 methylation occurs rapidly at the onset of random X chromosome inactivation. Curr. Biol. **12:**247–251.
44. **Chaumeil J, Okamoto I, Heard E.** 2004. X-chromosome inactivation in mouse embryonic stem cells: analysis of histone modifications and transcriptional activity using immunofluorescence and FISH. Methods Enzymol. **376:**405–419.
45. **Chamberlain SJ, Yee D, Magnuson T.** 2008. Polycomb repressive complex 2 is dispensable for maintenance of embryonic stem cell pluripotency. Stem Cells **26:**1496–1505.
46. **Rathert P, Dhayalan A, Murakami M, Zhang X, Tamas R, Jurkowska R, Komatsu Y, Shinkai Y, Cheng X, Jeltsch A.** 2008. Protein lysine methyltransferase G9a acts on non-histone targets. Nat. Chem. Biol. **4:**344–346.
47. **Fritsch L, Robin P, Mathieu JR, Souidi M, Hinaux H, Rougeulle C, Harel-Bellan A, Ameyar-Zazoua M, Ait-Si-Ali S.** 2010. A subset of the histone H3 lysine 9 methyltransferases Suv39h1, G9a, GLP, and SETDB1 participate in a multimeric complex. Mol. Cell **37:**46–56.
48. **Yokochi T, Poduch K, Ryba T, Lu J, Hiratani I, Tachibana M, Shinkai Y, Gilbert DM.** 2009. G9a selectively represses a class of late-replicating genes at the nuclear periphery. Proc. Natl. Acad. Sci. U. S. A. **106:**19363–19368.
49. **Bernstein E, Duncan EM, Masui O, Gil J, Heard E, Allis CD.** 2006. Mouse polycomb proteins bind differentially to methylated histone H3 and RNA and are enriched in facultative heterochromatin. Mol. Cell. Biol. **26:**2560–2569.
50. **Rasmussen TP, Wutz AP, Pehrson JR, Jaenisch RR.** 2001. Expression of Xist RNA is sufficient to initiate macrochromatin body formation. Chromosoma **110:**411–420.
51. **Ding Z, Gillespie LL, Paterno GD.** 2003. Human MI-ER1 alpha and beta function as transcriptional repressors by recruitment of histone deacetylase 1 to their conserved ELM2 domain. Mol. Cell. Biol. **23:**250–258.
52. **Sánchez C, Sánchez I, Demmers JA, Rodriguez P, Strouboulis J, Vidal M.** 2007. Proteomics analysis of Ring1B/Rnf2 interactors identifies a novel complex with the Fbxl10/Jhdm1B histone demethylase and the Bcl6 interacting corepressor. Mol. Cell. Proteomics **6:**820–834.
53. **Smits AH, Jansen PW, Poser I, Hyman AA, Vermeulen M.** 2013. Stoichiometry of chromatin-associated protein complexes revealed by label-free quantitative mass spectrometry-based proteomics. Nucleic Acids Res. **41:**e28. doi:10.1093/nar/gks941.
54. **Fischle W, Franz H, Jacobs SA, Allis CD, Khorasanizadeh S.** 2008. Specificity of the chromodomain Y chromosome family of chromodomains for lysine-methylated ARK(S/T) motifs. J. Biol. Chem. **283:**19626–19635.
55. **Wu H, Chen X, Xiong J, Li Y, Li H, Ding X, Liu S, Chen S, Gao S, Zhu B.** 2011. Histone methyltransferase G9a contributes to H3K27 methylation in vivo. Cell Res. **21:**365–367.
56. **Wan L, Hu XJ, Yan SX, Chen F, Cai B, Zhang XM, Wang T, Yu XB, Xiang AP, Li WQ.** 2013. Generation and neuronal differentiation of induced pluripotent stem cells in $Cdyl^{-/-}$ mice. Neuroreport **24:**114–119.
57. **Strahl BD, Allis CD.** 2000. The language of covalent histone modifications. Nature **403:**41–45.
58. **Turner BM.** 2000. Histone acetylation and an epigenetic code. Bioessays **22:**836–845.
59. **Schulze WX, Mann M.** 2004. A novel proteomic screen for peptide-protein interactions. J. Biol. Chem. **279:**10756–10764.